


February 2019

VOC Emission Factors from 3D Printers - ABS (Acrylonitrile-Butadiene-Styrene) Type Filaments

Dean Lay

Louisiana State University and Agricultural and Mechanical College

Follow this and additional works at: https://repository.lsu.edu/gradschool_theses

 Part of the [Analytical Chemistry Commons](#), [Environmental Health and Protection Commons](#), and the [Polymer Chemistry Commons](#)

Recommended Citation

Lay, Dean, "VOC Emission Factors from 3D Printers - ABS (Acrylonitrile-Butadiene-Styrene) Type Filaments" (2019). *LSU Master's Theses*. 4850.
https://repository.lsu.edu/gradschool_theses/4850

This Thesis is brought to you for free and open access by the Graduate School at LSU Scholarly Repository. It has been accepted for inclusion in LSU Master's Theses by an authorized graduate school editor of LSU Scholarly Repository. For more information, please contact gradetd@lsu.edu.

VOC EMISSION FACTORS FROM 3D PRINTERS – ABS (ACRYLONITRILE-BUTADIENE-STYRENE) TYPE FILAMENTS

A Thesis

Submitted to the Graduate Faculty of the
Louisiana State University and
Agricultural and Mechanical College
in partial fulfillment of the
requirements for the degree of
Master of Science

in

The Department of Environmental Sciences

by

Dean Lay

B.S., University of California, Davis, 2013

May 2019

Table of Contents

Acknowledgements	iii
Abstract.....	iv
1. Introduction	1
2. Literature Review	4
2.1. ABS Filament in 3D Printing.....	4
2.2. Health Effects of VOCs	10
3. Materials and Methods	17
3.1. Materials	17
3.2. The System for Thermal Diagnostic Studies (STDS)	17
3.3. Pyrolysis and Oxidative Pyrolysis	19
3.4. GC–MS Characterization	20
3.5. Mass Optimization	20
3.6. Calibration of Pyrolysis Products	21
3.7. Method Detection Limits.....	22
4. Results	23
4.1. Method Development	23
4.2. Pyrolysis of ABS and ABS-CNT	25
4.3. Oxidative Pyrolysis of ABS and ABS-CNT	28
5. Discussion.....	32
5.1. Mass Optimization	32
5.2. Degradation Mechanism	32
5.3. Effect of Carbon Nanotubes.....	33
5.4. Effect of Oxygen	36
5.5. Exposure Assessment	36
6. Conclusion	40
Appendix A. Tables of Emission Rates	43
Appendix B. Example Chromatograms	45
Appendix C. Permissions	50
References.....	51
Vita	58

Acknowledgements

I would like to acknowledge the following people for their help and contributions to this work:

Dr. Phillip Potter and Dr. Souhail Al-Abed at the United States Environmental Protection Agency for reaching out to our group at LSU for this collaborative research effort and enlisting me to develop the methodology and perform the experiments associated with it.

Dr. Slawo Lomnicki for mentoring me throughout this master's program, and frequently helping me realize that I was overthinking things.

Dr. Lavrent Khachatryan for help with troubleshooting and keeping the instrument running through all of my experiments.

Dr. Hayat Bennadji for teaching me how to use the instrumentation involved in this project and being a good role model in the laboratory.

Dr. Vincent Wilson and Dr. Kevin Armbrust for serving on my thesis committee and giving me advice along the way.

Abstract

Acrylonitrile-butadiene-styrene (ABS) is a polymer that is widely used in many plastic products and is receiving new attention due to its use as a filament for fused deposition modelling (FDM) 3D printers. It has been shown to emit potentially dangerous volatile organic compounds (VOCs) when heated at temperatures used in the 3D printing process. Many new products are becoming available that contain various additives to the polymer matrix, which have an unknown effect on the emission profiles and rates. In this study a method is developed using a modified system for thermal diagnostic studies (STDS) to evaluate VOC emission from ABS polymer at low temperature 3D printing conditions. Samples of pure ABS and ABS filament containing carbon nanotubes (CNTs) were analyzed by this instrument at 200°C, 230°C, and 300°C, for 1-minute and 3-minute heating times, under pure nitrogen and 4% O₂ carrier gases. The primary product detected for all reaction conditions was styrene. The majority of other detected VOCs were similar breakdown products of the polymer chain, such as ethylbenzene, α -methylstyrene, and isopropylbenzene, and their oxidized counterparts. The data suggests that the major effects of CNTs in the filament are to reduce emissions of styrene through the adsorption of monomers and to lower the amount of available matrix adsorbed oxygen. Oxygen in the carrier gas was shown to increase the proportion of oxidized products in the emission profile and decrease emissions of those without oxygen. The measured emission rates are consistent with studies that have analyzed VOC emissions from operating 3D printers, and do not identify significant risk associated with home use of the devices.

1. Introduction

With price tags down to almost \$200, 3D printers are now becoming a common household appliance. However, it has been shown their use produces measurable concentrations of both ultrafine particles and volatile organic compounds (VOCs)¹⁻⁵. This raises potential health concerns, especially if used around children and/or in small rooms without much ventilation. It is well established that both airborne particulate matter and VOCs can cause adverse health effects, such as eye, nose, and throat irritation, headaches, nausea, damage to liver, kidney, and central nervous system, and with some specific compounds, even cancer⁶⁻⁹. Many other consumer products also emit these types of pollutants¹⁰⁻¹³, and 3D printers are therefore an addition to an already growing problem of indoor air pollution. Moreover, some of the products identified as 3D printer emissions have very little toxicological data available. These compounds are in need of further study, as risk due to their exposure is largely unknown.

The release of VOCs from the heating of thermoplastic resins has been studied for decades¹⁴⁻¹⁶, and these types of polymers are commonly used by 3D printers in a process called fused deposition modelling^{17,18}. These older studies, however, are generally more focused on the thermal stability of the polymers rather than the VOC profile, and were carried out at higher temperatures than experienced in a 3D printer. Typical printing materials include polycarbonate, nylon, polyactic acid (PLA), and acrylonitrile-butadiene-styrene (ABS)¹⁷. ABS is one of the most frequently used of the

The data and ideas presented in the main body of this work are printed here with the permission of collaborators Phillip Potter, Souhail Al-Abed, and Slawomir Lomnicki.

group, likely due to its low cost and high durability, which allow it to be used in a variety of applications¹⁹.

The structure of ABS is a network of styrene and acrylonitrile monomers grafted onto polybutadiene, or a butadiene copolymer, which functions as an elastomer/rubber component²⁰, and is shown in Figure 1.1. The polymerization method and ratio of monomers can be varied in order to alter the properties of the resulting mixture^{15,20}. In addition, several types of additives can be included in the matrix to further enhance the properties of the resulting composite, such as brominated flame retardants, metal nanoparticles, and carbon nanotubes (CNTs)^{21,22}. The inclusion of CNTs increases the electrical and thermal conductivity of the matrix, as well as its tensile strength, which makes them useful for a variety of applications²³. However, little research has been done on the effect they have on the emission profile of ABS polymer when used in 3D printing.

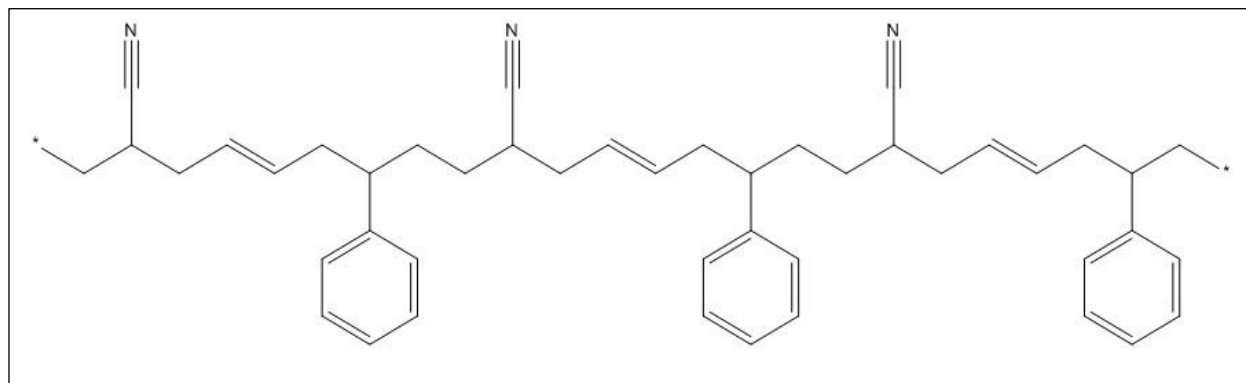


Figure 1.1. Typical chemical structure of ABS polymer.

This study focuses on the development of a method of identification and quantification of volatile organic compounds that are emitted from ABS polymer when heated under pyrolytic conditions and low-oxygen conditions. It aims to determine the effects of added carbon nanotubes, heating temperature, heating time, and the

presence of oxygen on the emission profile. Emissions from samples of filament designed for use in a 3D printer with and without CNTs in the matrix have been captured and analyzed by GC/MS.

2. Literature Review

2.1. ABS Filament in 3D Printing

2.1.1. History and Applications of 3D Printing

The patent for what is now commonly known as a 3D printer was filed in 1992 by Scott Crump¹⁸. It describes the design and application for a device which uses “a movable dispensing head provided with a supply of material which solidifies at a predetermined temperature, and a base member, which are moved relative to each other along ‘X’, ‘Y,’ and ‘Z’ axes in a predetermined pattern to create three-dimensional objects by building up material discharged from the dispensing head onto the base member at a controlled rate.” This process of fused deposition modelling is the most common type of 3D printing used in homes, offices, and schools, due to its low cost, high speed, and relative simplicity¹⁷.

A paper by Conner et al.²⁴ explores products and services associated with 3D printing, and looks at its advantages compared to conventional manufacturing. These include the creation of parts with complex geometry, printing whole objects that would otherwise need to be made in parts and assembled later, the ability to easily create prototypes from computer models, and the ability to customize products to the individual consumer. However, it generally falls short of conventional manufacturing when it comes to mass production of a large number of objects²⁴. Due to this, 3D printers are more often used in offices, laboratories, libraries, and schools, rather than on large assembly floors. When talking about exposure to emissions, this introduces the scenario of traditional indoor air pollution, in addition to occupational exposure.

2.1.2 Emissions from Fused Deposition Modelling of 3D Printers

In the past decade an effort has begun to examine the emissions from desktop 3D printers. Studies are being performed that collect, identify, characterize, and quantify particles, aerosols, and VOCs that are released during printing, using a variety of methods. Stefaniak et al.³ placed a 3D printer in a stainless steel chamber with conductive carbon and stainless steel sampling tubes and printed a small hair comb using different filaments. Air from the chamber was collected in 6-liter canisters and later analyzed by GC-MS for VOCs. Detected compounds while printing with ABS polymer were: acetaldehyde, ethanol, acetonitrile, acetone, isopropanol, n-hexane, chloroform, benzene, toluene, ethylbenzene, m,p-xylene, styrene, and o-xylene. The presence and distribution of these products differed based on the color of the filament, with styrene as the most abundance VOC in each sample. Based on the levels measured, they estimated that 8 hours of printing from a single printer in a 40 m³ room without ventilation would generate a TVOC concentration ranging from 215–710 µg/m³.

A study by Patrick Steinle⁴ used a 3D printer in an 85 L acrylic glass hood on top of a steel plate to print a 16.75 g object, taking approximately 165 minutes to complete. VOCs were captured on Tenax adsorbent tube and analyzed by thermodesorption GC-MS. The major products identified in the samples printed with ABS were styrene, ethylbenzene, cyclohexanone, n-butanol, and methyl-methacrylate. Emission rates of TVOCs and styrene were calculated as 100 and 58 µg/g, respectively. In addition, Steinle looked at indoor air concentrations in a large ventilated room (180 m³) and a small unventilated room (30 m³) when a desktop printer was operating (though using PLA filament rather than ABS). The mean TVOC concentrations were 33 and 216

$\mu\text{g}/\text{m}^3$, respectively, 2.5 m away from the printer, near the end of the printing time of the object.

Floyd, Wang, and Regens⁵ placed their 3D printer in a 24.8 L enclosed transparent glass box chamber. Volatile emissions were collected on tri-sorbent sampling tubes while a small object with a print time of 75 minutes was produced in the chamber. Samples were analyzed by thermal desorption GC-MS. A full speciated list of VOCs is not presented, however, styrene, α -methyl styrene, ethylbenzene, and acetophenone were listed as major products. The calculated emission rates while printing with ABS were $63.9 \mu\text{g}/\text{min}$ ($782.1 \mu\text{g}/\text{g}$) for total VOCs and $4.8 \mu\text{g}/\text{min}$ for styrene.

2.1.3. Properties and Synthesis of ABS Polymer

There are a variety of different polymers used in fused deposition modelling, but ABS is the most versatile and therefore one of the most common¹⁹. It is an amorphous polymer composed of a butadiene elastomer acting as the rubber component and a styrene-acrylonitrile (SAN) copolymer as the thermoplastic matrix. Butadiene is dispersed in the matrix as grafted particulates, which can vary in size and distribution based on the processing method. This blend of polymeric components exhibits excellent toughness, chemical resistance, stability, and processability. The particle size, morphology, microstructure, graft structure, and SAN composition can all be manipulated to alter the properties of the final mixture²⁰.

The rubber/elastomer component is generally the product of free-radical polymerization of butadiene, either through thermal or redox reactions. 1,4-polybutadiene is the main product, with 1,2-polybutadiene as the second most abundant²⁰. Cross-linking will occur during this process and can be controlled with

chain-transfer agents and the concentration and type of initiator. Chain transfer agents are compounds that are used to control the length of individual polymer chains, and examples include halogenated hydrocarbons, thiols, and mercaptans²⁵. This is accomplished through hydrogen abstraction from a transfer agent to a growing polymer chain, thereby ending the polymerization of the chain, but continuing to propagate the radical through the agent²⁶. Radical chain initiators are compounds such as peroxides and azo compounds which can form radicals when heated and begin the radical chain polymerization of the desired monomers²⁷.

Grafting is a free-radical process that involves cross-linking of the SAN polymer with the butadiene elastomer particles. This happens through both hydrogen abstraction and copolymerization of double bonds. Its extent can be modified through the same methods as described above for cross-linking of polybutadiene²⁰.

There are 3 main methods of ABS synthesis: Emulsion, mass polymerization, and suspension. Emulsion involves a two-stage reaction in water, in which the elastomer is polymerized first, then styrene and acrylonitrile are grafted on in a second step. The use of water reduces the viscosity and allows for the creation of ABS with a wide range of rubber content, including amounts higher than possible with other polymerization techniques. However, it generates more wastewater and uses more energy. Mass polymerization is usually performed by dissolving linear polybutadiene in a solution of styrene and acrylonitrile monomers. This process results in larger rubber particles and less total rubber content than the emulsion process and has a final product that looks more translucent. The suspension process starts with either of the other two but stops the reaction at 15-30% conversion and suspends the mixture in water with a

suspending agent. This gives a similar product to the mass polymerization process, but has some of the processing advantages associated with emulsion due to the use of water²⁰.

2.1.4. Carbon Nanotubes as Polymer Additives

An optional step in the production of ABS polymer is the inclusion of additives into the matrix through compounding. This can be done on several types of equipment, such as melt mixers and screw extruders. Wang et al.¹⁷ wrote a review article on 3D printing with different polymer matrix composites, including particles made of glass or metal, carbon fibers, and nanocomposites using metals, ceramics, graphite, graphene, and carbon nanotubes. In addition, specific applications for these technologies were discussed, such as the printing of tissues and organs, printing of electrically conductive materials, and printing of aerospace materials.

Carbon nanotubes are cylinders of rolled sheets of crystallized carbon, a single atom thick. The typical diameter is around 1.4nm, though this can vary slightly. Due to this variation in diameter, multi-walled structures can form with smaller units fitting inside of larger ones. Three different types of structures exist based on the chiral angle, known as armchair, zigzag, and chiral nanotubes²⁸. They can be grown through a variety of methods, including arc-discharge, laser ablation, and chemical vapor deposition²⁹.

CNTs are a particularly versatile additive in ABS polymers, as they increase electrical conductivity, mechanical strength, and thermal stability^{22,30}. A recent study by Dul, Fambri, and Pegoretti²³ showed that increasing CNT content in ABS polymers decreased the melt flow index, increased bulk density, increased tensile modulus and yield strength, enhanced the storage modulus and dissipation of mechanical energy,

increased the glass transition temperature, and reduced the coefficient of thermal expansion. The maximum degradation temperature increased with up to 2% CNTs, then decreased with inclusion of 4 to 8% CNTs.

However, Yang, Castilleja, Barrerra, and Lozano³¹ showed back in 2004 that the addition of single walled carbon nanotubes (SWNTs) accelerated the initial degradation of ABS during thermogravimetric analysis (TGA). They suggested that the nanotubes take part in the initiation of the decomposition process and are degraded as well. The temperature of the second degradation step was increased by inclusion of a small amount of SWNTs (0.5 to 3.5%), but then reduced at the larger concentrations of 5 and 10%.

2.1.5. Thermal Decomposition of Polymers

The American Society for Testing and Materials (ASTM) defines thermal decomposition as a “process whereby the action of heat or elevated temperature on an item causes changes to the chemical composition”³². This generally involves the volatilization of relatively small molecules from the substrate. For polymeric materials, these smaller molecules are often comprised of monomers that break off from the nonvolatile chain. The rate and mechanism of this decomposition is influenced by the chemical and physical properties of the polymer, including their degree of crystallinity, molecular weight, prior thermal damage, weak linkages, and primary radicals³³.

There are four main mechanisms of decomposition for polymers: Random-chain scission, end-chain scission, chain-stripping, and cross-linking. These occur in varying degrees based on the structure of the polymer, and usually more than one is relevant for a specific polymer. The process is dominated by radical chain reactions and is the reverse of the polymerization reaction. Heat energy causes a bond to break, forming a

free radical. That radical is then able to abstract a hydrogen from somewhere else, either in its own polymer chain or a neighboring one, creating a new radical. The location of the removed hydrogen is largely impacted by the structure of the polymer, with steric hindrance being very important. Large side groups surrounding a radical generally lead to intramolecular transfer, and “unzipping”, in which the terminal group is removed and a new terminal radical is formed³³.

Thermal decomposition of ABS polymer has been investigated in many studies using different methodologies, including TGA, derivative thermogravimetry (DTG), differential scanning calorimetry (DSC), and gas-chromatography (GC) with various detectors^{15,16,34,35}. GC analysis has identified the following major degradation products of ABS polymer: acrylonitrile, 1,3-butadiene, hydrogen cyanide, 4-vinylcyclohexene, ethylbenzene, styrene, isopropylbenzene, propylbenzene, methyl styrene, acetophenone, 2-phenyl-1-propanol, benzaldehyde, and phenol, as well as small volatiles such as alcohols, aldehydes, and saturated hydrocarbons^{14,15,36,37}.

2.2. Health Effects of VOCs

There were eleven VOCs in this study that were detected from ABS decomposition and quantified. In Table 2.1 below, these compounds are listed along with their reported symptoms of acute and chronic exposure. Some of these compounds, such as 2,4-di-tert-butylphenol and 2-phenyl-2-propanol, do not have much data available, while others, like styrene, have been studied extensively. Those with a lack of toxicological data are concerning, as their effects on humans are therefore largely unknown and could pose additional threats that have yet to be identified. In addition, many of these products share some of the same effects for inhalation

exposure, such as irritation of the respiratory airways and CNS depression, meaning that they could have additive or even synergistic effects. The toxicity of mixtures is a topic that still holds many uncertainties and requires extensive research to properly investigate.

Table 2.1. Acute and chronic effects associated with exposure to major products of ABS degradation through different routes of exposure

Compound	Acute Effects	Chronic Effects
Acetophenone ^{38,39}	<p><u>Oral</u>: Sedative effects, hematological effects, coma</p> <p><u>Inhalation</u>: Congestion of lungs, kidney, and liver</p> <p><u>Dermal</u>: Skin irritation, corneal injury</p>	<p><u>Inhalation</u>: Degeneration of olfactory bulb cells, hematological effects, congestion of cardiac vessels</p>
Benzaldehyde ⁴⁰⁻⁴²	<p><u>Oral</u>: Depression, tremors, intestinal irritation, hemorrhage, coma</p> <p><u>Inhalation</u>: Decrease in respiratory rate</p> <p><u>Dermal</u>: Edema, erythema, eschars, necrosis</p>	<p><u>Inhalation</u>: Respiratory airway irritation, CNS impairment (Subchronic)</p> <p><u>Dermal</u>: Ocular irritation, dermal irritation</p>
Cumene (Isopropyl benzene) ⁴³⁻⁴⁵	<p><u>Inhalation</u>: Headaches, dizziness, unconsciousness, CNS depression.</p> <p><u>Dermal</u>: Skin and eye irritation</p> <p><u>Intravenous</u>: Excitation of vestibulo-oculomotor reflex</p>	<p><u>Oral</u>: Increase in kidney weight.</p> <p><u>Inhalation</u>: Increase in liver, kidney, and adrenal weight.</p>
2,4-di-tert-butylphenol ⁴⁶⁻⁴⁸	<p><u>Dermal</u>: Vitiligo, erythema, edema, hemorrhage of dermal capillaries</p>	<p><u>Oral</u>: Growth retardation, hepatotoxicity, renal toxicity</p>
2,6-di-tert-butylquinone ⁴⁹	<p><u>Not specified</u>: Convulsions, medullary paralysis</p>	<p><u>Not specified</u>: Neurotoxicity, vision disturbances</p>

(table cont'd)

Compound	Acute Effects	Chronic Effects
Ethylbenzene ^{44,50,51}	<u>Oral</u> : Damage to inner ear <u>Inhalation</u> : Eye and throat irritation, vertigo, dizziness <u>Dermal</u> : Eye damage and skin irritation	<u>Inhalation</u> : Damage to inner ear and hearing, kidney damage, kidney, lung, and liver tumors
α -methylstyrene ^{44,52}	<u>Inhalation</u> : Irritation of upper respiratory tract. <u>Dermal</u> : Irritation of eyes and skin. <u>Intravenous</u> : Excitation of vestibulo-oculomotor reflex	<u>Inhalation</u> : CNS depression
2-phenyl-2-propanol ^{53,54}	<u>Inhalation</u> : Headache, dizziness, tiredness, nausea, vomiting	<u>Not specified</u> : Increase in leukocytes, reduced hemoglobin content, increased activity of aminotransferase
Styrene ^{44,55-57}	<u>Inhalation</u> : Impaired vestibular function	<u>Inhalation</u> : Decreased color discrimination, hearing impairment, feeling drunk, tiredness, delays in reaction time, impaired attention and memory
TMSN ^{58,59}	<u>Inhalation</u> : Convulsions, loss of consciousness	<u>Inhalation</u> : headaches, excessive salivation and sense of taste, nausea, vomiting, dizziness, respiratory distress
4-vinylcyclohexene ⁶⁰⁻⁶²	<u>Inhalation</u> : keratitis, rhinitis, headache, hypotonia, leukopenia, neutrophilia, lymphocytosis <u>Dermal</u> : Irritation	<u>Intraperitoneal</u> : Ovotoxicity – cell death of follicles <u>Inhalation</u> : Lethargy, tremors, ovarian atrophy

There is also evidence suggesting that some compounds in this list can cause cancer. Styrene is listed by the International Agency for Research on Cancer (IARC) as group 2A, probably carcinogenic to humans, and α -methylstyrene, ethylbenzene, 4-

vinylcyclohexene, and isopropyl benzene are in group 2B, possibly carcinogenic to humans⁷.

2.2.1. Risk Assessment

Based on the products that have been identified as emissions from ABS filament, it seems that there is potential harm associated with the use of 3D printers. This potential harm can be evaluated and quantified through the process of a human health risk assessment. Many governmental agencies such as the US EPA have guidelines on how to perform such an assessment^{63,64}. In short, this is done by identifying the potential hazards, assessing the dose-response relationships of the pollutants, assessing the potential exposure, and then characterizing the risk, both quantitatively and qualitatively. The process involves gathering information about what a population is exposed to, where they are exposed, how they are exposed, and how much they are exposed. This is all combined with information about how dangerous or toxic the substances involved are, to calculate values for risk using regulatory reference values.

The current study contributes to identification of the hazards and assessment of exposure. A 3D printing exposure scenario is based on the inhalation of contaminated indoor air model. There are many sources of indoor air pollutants aside from those related to 3D printers, including fuel-burning appliances, tobacco products, building materials, consumer care products, etc¹⁰. If not properly controlled, these can individually or cumulatively create unsafe conditions for human health. People are increasingly spending more time indoors⁶⁵, which increases exposure time and the risk of adverse health effects. Therefore, gathering information on emission rates of indoor air pollutants is becoming increasingly important. These values are needed to create

realistic exposure scenarios, which can then be combined with the available toxicological data to calculate accurate risk values.

An example of these regulatory values for acute exposure are the Protective Action Criteria (PAC) organized by the United States Department of Energy. These include Threshold Limit Values (TLVs) from the American Conference of Governmental Industrial Hygienists (ACGIH), Temporary Emergency Exposure Limits (TEELs), Workplace Environmental Exposure Levels (WEELs), Emergency Response Planning Guidelines (ERPGs), and Short-Term Exposure Limits (STELs), set by the American Industrial Hygiene Association (AIHA), as well as Acute Exposure Guideline Levels (AEGs) set by the US Environmental Protection Agency (EPA). They are likely relevant to a 3D printing scenario where many printers are operating at once in the same room, for example where prototypes are being developed in an office. Table 2.2 presents these values for compounds identified in this study. Three of these do not have regulatory values and are represented in the table by other compounds with similar structures.

For the scenario of a single 3D printer in an office or home, values based on chronic exposure are better suited for risk assessment. The primary values used for this purpose are the United States Environmental Protection Agency's (US EPA) Reference Dose (RfD) and Reference Concentration (RfC), for oral and inhalation exposures, respectively. Table 2.3 lists values for major products of ABS degradation where they are available.

Table 2.2. Protective Action Criteria for major products identified in this study⁶⁶.

Compound	PAC-1	PAC-2	PAC-3
Acetophenone	30 mg/m ³ TLV-TWA	87 mg/m ³ TEEL-3/6	520 mg/m ³ Rat oral LD ₅₀
Benzaldehyde	4 ppm WEEL-STEL	9.9 ppm TEEL-3/6	59 ppm Rat oral LD ₅₀
Cumene (Isopropyl benzene)	50 ppm AEG1-1	300 ppm AEG1-2	730 ppm AEG1-3
Ethylbenzene	33 ppm AEG1-1	1100 ppm AEG1-2	1800 ppm AEG1-3
α-methylstyrene	100 ppm REL-STEL	830 ppm TEEL-3/6	5000 ppm IDLH (1990)
2-phenyl-2-propanol	0.7 ppm TEEL-2/11	7.7 ppm TEEL-3/6	46 ppm Rat oral LD ₅₀
Styrene	20 ppm AEG1-1	130 ppm AEG1-2	1100 ppm AEG1-3
4-vinylcyclohexene	0.3 ppm TLV-TWA x 3	210 ppm Rat 360-min TCLo	340 ppm Rat 240-min LCLo
Azobis (2- methylpropionitrile), 2,2'-*	4.1 TEEL-2/11	45 Rat oral TDLo	130 Rat oral LD ₅₀
2,5-Di-tert- butylhydroquinone**	6.3 mg/m ³ TEEL-2/11	69 mg/m ³ Rat oral TDLo	110 mg/m ³ Mouse oral LD ₅₀
4-tert-butylphenol***	1.5 mg/m ³ MAK-TWA x 3	40 mg/m ³ TEEL-3/6	240 mg/m ³ Rat 240-min LCLo

* Listed as a surrogate for tetramethylsuccinonitrile

** Listed as a surrogate for 2,6-di-tert-butylquinone

*** Listed as a surrogate for 2,4-di-tert-butylphenol

Table 2.3. US EPA reference concentration or reference dose for major products identified in this study.

Compound	RfC or RfD
Acetophenone ⁶⁷	RfD = 0.1 mg/kg-day
Benzaldehyde ⁶⁸	RfD = 0.1 mg/kg-day
Cumene ⁶⁹ (Isopropyl benzene)	RfC = 0.4 mg/m ³
Ethylbenzene ⁷⁰	RfC = 1 mg/m ³
Styrene ⁷¹	RfC = 1 mg/m ³

3. Materials and Methods

3.1. Materials

The polymer samples were obtained from the USEPA Office of Research and Development and used without further treatment. They were purchased from 3DXTech and have since been discontinued. The nanotube containing samples were experimentally determined by the EPA to be approximately 1% CNT by weight. The quartz sample baskets were made in the LSU Chemistry Department glassblowing shop. HPLC grade dichloromethane (DCM) was purchased from Fisher Scientific. Pure compounds used for calibration were purchased from Sigma Aldrich and dissolved in dichloromethane to create standard solutions.

3.2. The System for Thermal Diagnostic Studies (STDS)

Rather than capture emissions directly from 3D printing, as done in studies such as Steinle 2016⁴, the system for thermal diagnostic studies (STDS) was used for this analysis. The system used in this study has been modified from the original design, which was described by Rubey and Grant in 1988⁷². The modified system consists of a vertical tubular quartz reactor (7 mm internal diameter, 110 mm length, 20 mm isothermal zone) suspended in a GC oven, which contains a ceramic furnace heated by a thermocouple attached to an external controller. A tank of carrier gas is attached to the reactor through a mass flow controller. All gaseous products released from the heating of a sample in the reactor are taken by the carrier gas through a heated transfer line into the inlet of another gas chromatograph that is cooled to -60°C with liquid nitrogen, and subsequently analyzed by mass spectrometry. This system allows for a closer look at the fundamentals of ABS pyrolysis/oxidative pyrolysis, as all volatile and

semi-volatile products are captured and analyzed. The most important difference from the original design is the use of a vertical reactor with a movable sample holder. This change allows for samples to be rapidly introduced into a pre-heated furnace, rather than subjecting them to a temperature ramp, better matching the heating conditions inside of an extruder nozzle. The reactor used in this work is presented in Figure 3.1. Collection was done in an Agilent 6980 GC at the head of a DB-5ms column and analysis was carried out by an Agilent 5973N mass spectrometer. The transfer line temperature was held at approximately 280°C.

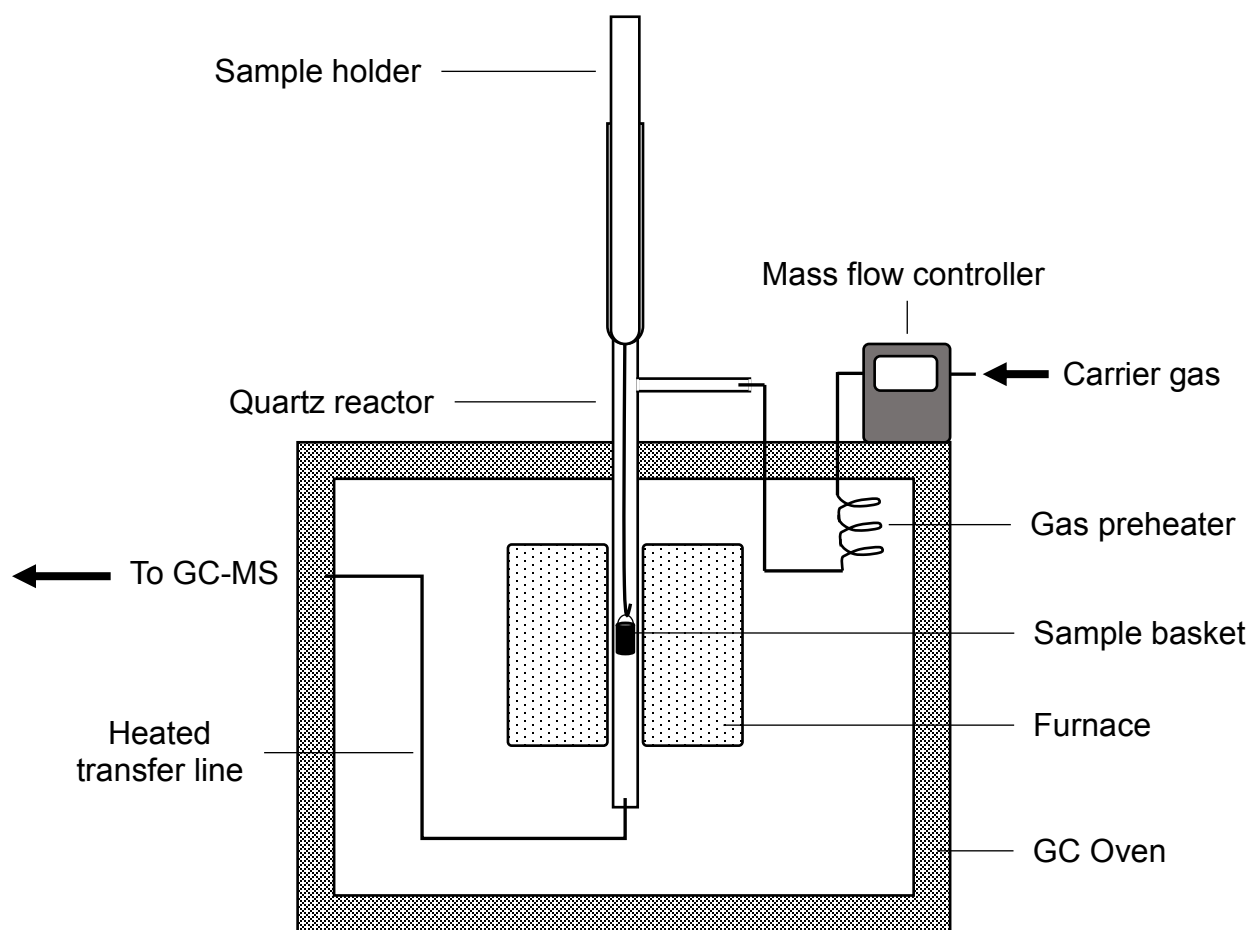


Figure 3.1. Schematic diagram of STDS reactor.

3.3. Pyrolysis and Oxidative Pyrolysis

This experiment used conventional pyrolysis, with a fresh sample pyrolyzed for each product collection. Polymer samples were heated in the vertical quartz tube reactor under pure nitrogen flow at 200°C, 230°C, and 300°C, and under 4% oxygen in nitrogen flow at 230°C, and 300°C, for 3-minute and 1-minute reaction times. These temperatures and heating times were based on manufacturers' recommendations for extruder nozzle temperature and filament feed rate⁷³⁻⁷⁷. While 300°C is considerably higher than any recommended set point, this temperature is included to reflect the often-uneven heating of the nozzle. A low concentration of oxygen was used for oxidative pyrolysis to simulate estimated conditions inside the extruder of a 3D printer. During printing, melted filament flows through the extruder, filling the available volume and likely preventing much contact with air until it exits the nozzle. The gas flow rate was altered at each temperature to maintain a constant vapor residence time in the reactor of 0.2 seconds, minimizing secondary reactions.

Samples were generally 50 ± 2.5 mg, with the exception of the 1-minute pyrolysis samples at 100 ± 2 mg. They were loaded into small quartz (15 mm x 4 mm i.d.) baskets with a closed bottom and hung in the tubular reactor. Excess oxygen was purged from each pyrolysis sample by hanging in the path of the gas flow outside of the heated zone for 3 minutes. Next, the basket was lowered into the furnace for the specified reaction time. Finally, the sample was removed from the furnace and cooled under the gas flow, and the mass was measured and recorded. Blank samples consisting of an empty basket were analyzed to check for any carryover of products sticking to the column or transfer line.

3.4. GC–MS Characterization

Analysis of the gas phase emissions was conducted using an Agilent 6890N gas chromatograph equipped with a 5973N mass selective detector (MSD) with an electron impact (EI) ion source set at 70 eV. The installed column was a DB-5ms (30 m x 0.25 mm x 0.25 μ m). The temperature program was as follows: -60°C initial temperature held for 0.5 min, followed by heating at a rate of 15°C/min to 130°C, held for 1 min, heated to 225°C at a rate of 25°C/min, and finally heated to 300°C at 10°C/min and held for 7 minutes, giving a total runtime of 32.47 minutes. The split/splitless inlet of the GC was set to 280°C with a constant split flow of 10 mL/min. The carrier gas used was Ultra High Purity Helium (UHP, 99.999%) at a constant column flow of 1.0 mL/min. However, during sample collection the flow of nitrogen through the transfer line was high enough to increase the column flow to 2mL/min or above, with the rest going out the split vent. The mass spectrometer was operated in total ion current mode (TIC) over a mass scan range of 50–500 amu. Identification of volatile products was performed using the Wiley and NIST libraries and by comparison of retention times with those of purchased standard compounds.

3.5. Mass Optimization

Before settling on 50 mg as the optimum sample mass for this experiment, other values were tested. A small sample of 5 mg was initially tested in order to confirm that the emissions collected were not in a range that would overload the mass spectrometer. The mass was then increased to 10, 25, and 50 mg and the effect of this increased sample size on the instrument response values was evaluated. As the peak area values were not near levels that would overload the detector, the mass of 50 mg was used for

3-minute runs and doubled to 100 mg for 1-minute runs, to increase response of detected compounds.

3.6. Calibration of Pyrolysis Products

A stock solution was prepared by measuring out approximately 250 mg of each individual calibration compound and dissolving together in HPLC grade DCM in a 25 mL volumetric flask. Aliquots of the 10,000 µg/mL stock solution were then diluted to concentrations of 1,200, 800, 500, 200, and 50 µg/mL. For the two products in highest abundance, styrene and 2,4-di-tertbutyl-phenol, 500 mg was used instead, giving double the concentration of all other analytes. Emissions of 2,6-di-tert-butylquinone were approximated using the standard for 2,4-di-tertbutyl-phenol.

One microliter of each standard solution was injected into the GC–MS and calibration curves were constructed for each individual compound. Peak areas were adjusted for the 1:10 split ratio in the GC inlet and were plotted against mass injected, calculated from the known concentrations. All R^2 values for linear regressions of the standard curves were greater than 0.94. Product yields were calculated in µg from these regressions after correction for the split ratio calculated during sampling. This was the total flow from the transfer line, plus the 10 mL/min split flow, divided by the measured flow through the column. The value was generally in the range of 50:1. Emission rates in µg/g for each product were calculated by dividing the product yield by the approximate mass of the sample (50mg or 100mg). Emission values reported in this study are averages from either 2 or 3 replicates.

3.7. Method Detection Limits

Method Detection Limits (MDLs) were determined for each compound in the standard mix. Solutions with concentrations near the estimated detection limit were prepared on three separate days and analyzed a total of seven times. The heated transfer line and the 4% O₂ cylinder were connected to the inlet of the GC containing the reactor. One microliter of solution was injected through this inlet, allowing it to pass through the transfer line into the inlet of the analytical GC-MS, where it was collected at -60°C for approximately 3 minutes. The gas flow was set to match the rate during sample collection. MDLs were calculated by taking the standard deviation of measured concentration for each compound and multiplying by the Student's t-value for a single-tailed 99th percentile t-statistic with 6 degrees of freedom. Some analyzed samples contained peaks for which the concentration was calculated as being below the method detection limit. These values are flagged in any figures in which they appear to indicate that the reported concentrations are estimates.

4. Results

4.1. Method Development

When testing samples to determine the optimum mass, five compounds were detected at all three temperatures: Styrene, ethylbenzene, 4-vinyl-cyclohexene, 2-phenyl-2-propanol, and isopropyl benzene. The three different temperatures tested (200°C, 230°C, and 300°C) showed slightly different trends in response with increasing sample mass. For a heating time of 3 minutes, the increase in response for the sum of these major products was approximately 75% for 10 mg compared to 5 mg at 300°C, 25%, 50%, and 55% for ~25 mg compared to 10 mg at 200°C, 230°C, and 300°C, respectively, and 75%, 70%, and 20% for 50 mg compared to 25 mg at 200°C, 230°C, and 300°C, respectively. Figure 4.1 shows the approximate mass versus peak area count for these samples.

For pyrolysis samples with a heating time of 1 minute, 100 mg was used to increase the amount of volatiles collected and boost instrument response. However, this did not have as great of an effect as intended, and below 300°C only two major products were detected. Due to this, and the increased difficulty of removing the larger samples from the basket, the 1-minute oxidative pyrolysis samples were analyzed using a series of three 50 mg samples captured on the column one after the other and analyzed by the MS as one sample.

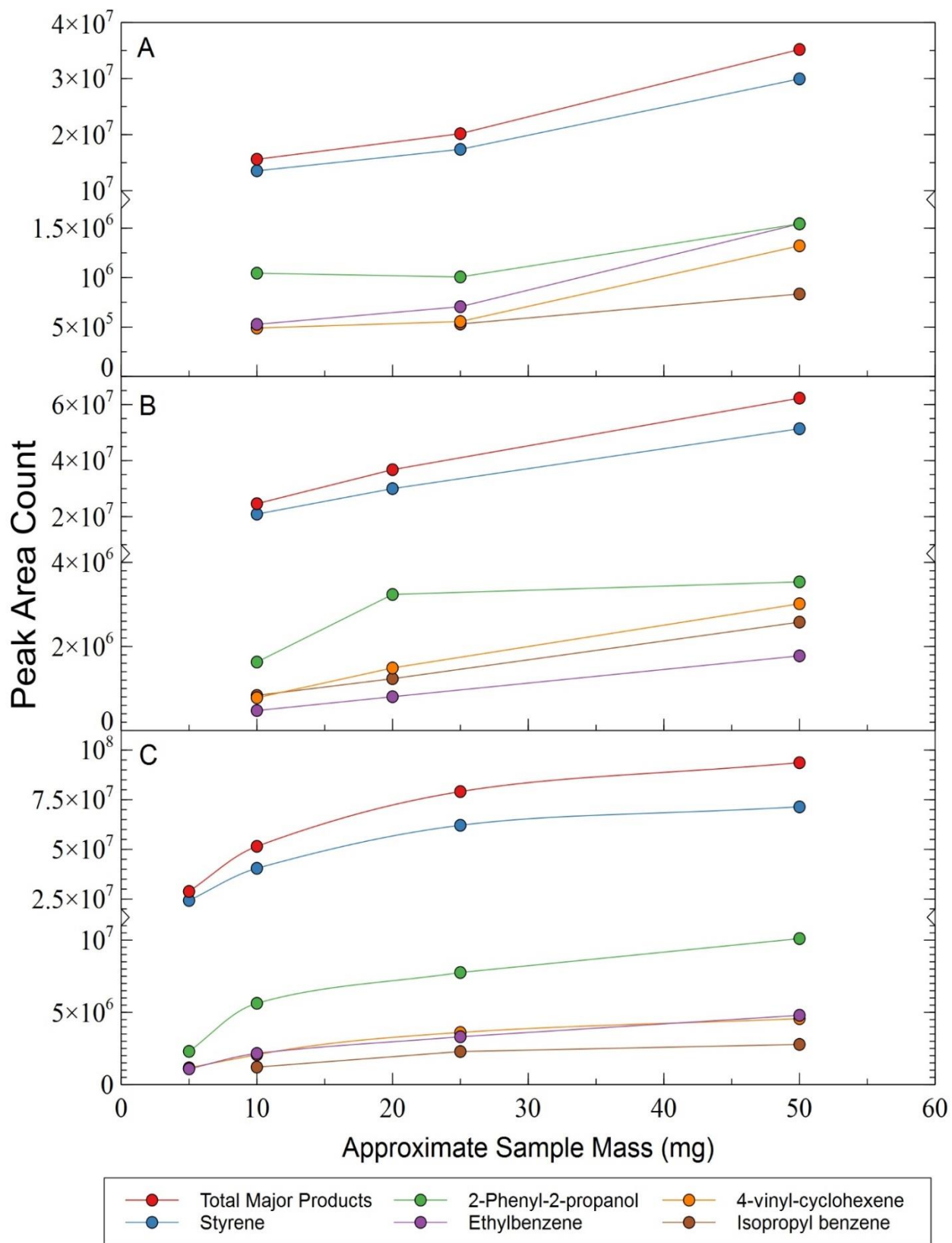
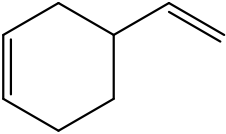
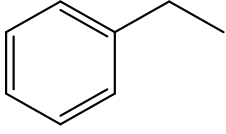


Figure 4.1. Sample mass vs peak area at 200°C (A), 230°C (B), and 300°C (C)

4.2. Pyrolysis of ABS and ABS-CNT

While the mass loss for each sample run in the experiment was less than 1%, volatile and semi-volatile products were detected at measureable levels for each reaction condition. The identified major products of pyrolysis are listed along with their source and structure in Table 4.1. These are the products that were in relatively high abundance, could be identified through the spectral library, and are of toxicological significance. Smaller molecular weight products that may also be toxicologically relevant were not identified due to poor separation on the GC-MS column. Other small peaks that could not be confidently identified were present in the chromatograms, with many of them likely being alkanes of different lengths and ring structures. Additionally, three large peaks towards the end of the chromatogram were poorly separated and could not be identified. They shared the principal ions of m/z 129 and 156, were likely nitrogen containing aromatics, and are an area for further investigation.

Table 4.1. Major identified products, their proposed source, and their chemical structure, listed in order of retention time.

Compound	Source	Structure
4-Vinylcyclohexene	Butadiene monomer dimerization	
Ethylbenzene	Polymer backbone cleavage	

(table cont'd)

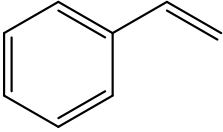
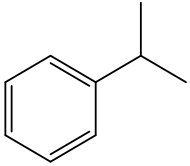
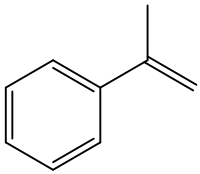
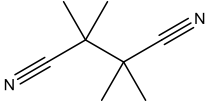
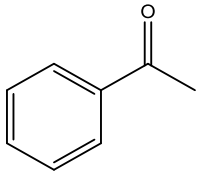
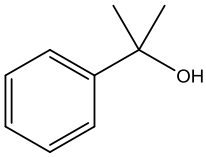
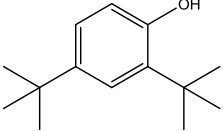
Compound	Source	Structure
Styrene	Unreacted monomer / backbone cleavage	
Isopropylbenzene	Polymer backbone cleavage	
α -Methylstyrene	Polymer backbone cleavage	
Tetramethylsuccinonitrile	Polymerization byproduct	
Acetophenone	Oxidation of backbone cleavage intermediate	
2-Phenyl-2-propanol	Oxidation of backbone cleavage intermediate	
2,4-Di-tert-butylphenol	Polymer UV-stabilizer component	

Figure 4.2 shows the emissions in $\mu\text{g/g}$ of each major pyrolysis product from ABS filament at the three tested temperatures, for both 3- and 1-minute heating times. There is a clear trend in each case of increasing emission with increasing temperature and

with increased heating time. For 3-minute reactions, acetophenone was not detected at 200 or 230°C, and was only detected in one of three samples analyzed at 300°C. Tetramethylsuccinonitrile (TMSN) was not detected at 200°C, and α -methylstyrene was only detected at 300°C. For the 1-minute reactions, styrene was the only product detected at temperatures of 200 and 230°C, and acetophenone and α -methylstyrene were not seen at all. 2,4-di-tert-butyl phenol was not detected from ABS polymer at any temperature or reaction time.

ABS-CNT filament showed the same overall trend of increasing emissions with increasing temperature and reaction time, with a slightly different distribution of products. Styrene was still the dominant product formed, however generally in smaller quantities compared to ABS without nanotubes. The second most abundant product changed from 2-phenyl-2-propanol to a compound not seen in ABS—2,4-di-tert-butylphenol. In addition, there was a significant increase in TMSN and α -methylstyrene. Direct comparisons of products between ABS and ABS-CNT are shown in Figure 4.3.

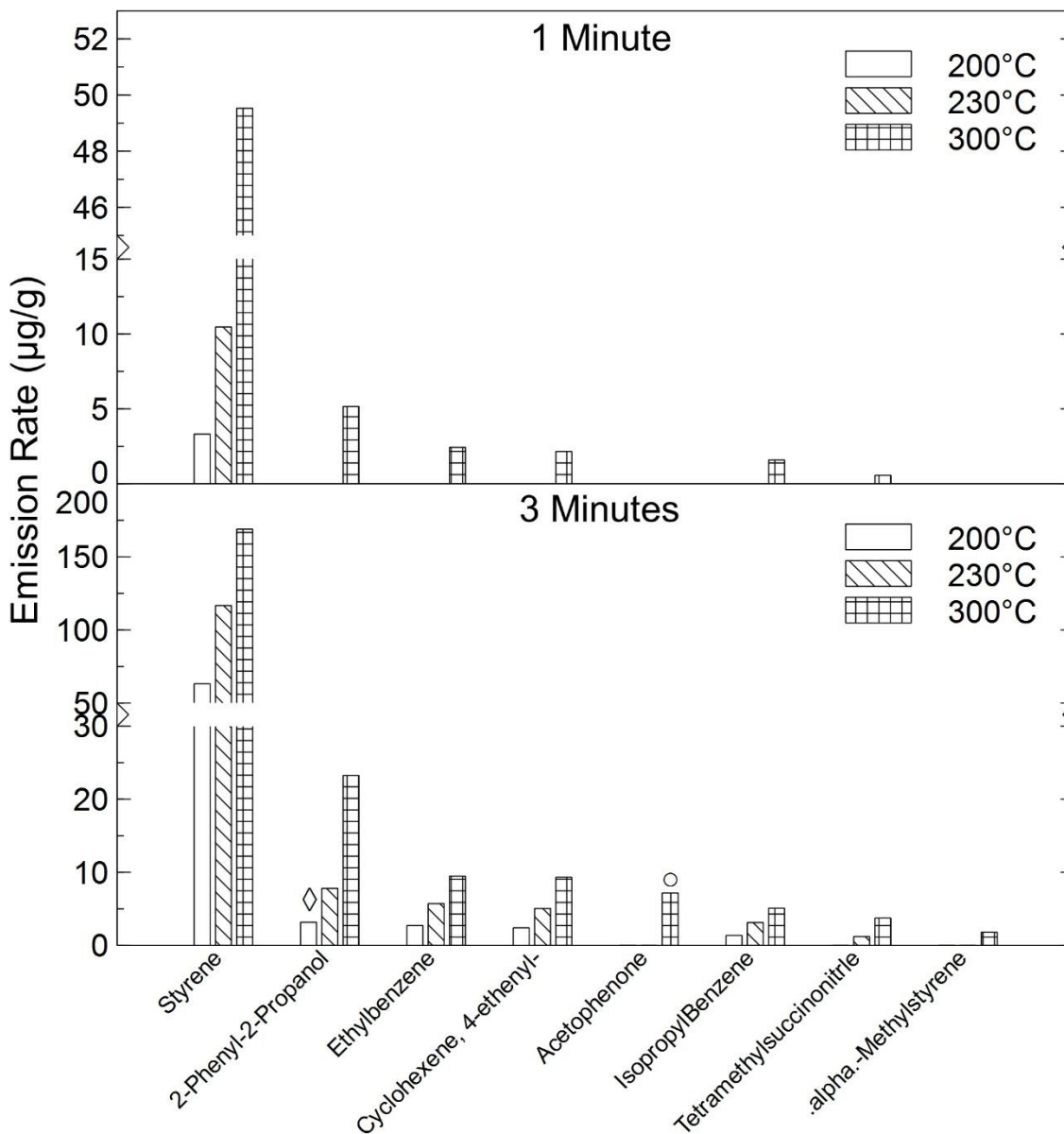


Figure 4.2. Emission rates of VOCs from ABS polymer at 200°C, 230°C, and 300°C for 1-minute (A) and 3-minute (B) reactions. ◇ = Below calculated MDL. ○ = Value equals one detection averaged with two 0.5*MDLs

4.3. Oxidative Pyrolysis of ABS and ABS-CNT

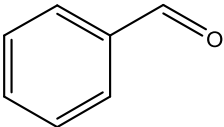
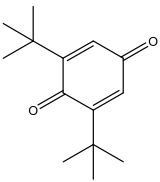
Figure 4.3 presents the emission rates of ABS and ABS-CNT filament at 230°C and 300°C, under pyrolysis and 4% O₂ conditions, for 3-minute samples. When oxygen was introduced to the reaction, two new major products were detected: Benzaldehyde and 2,6-di-tert-butylquinone. Their structures and sources are shown in Table 4.2. At a

reaction time of 3 minutes and a temperature of 300°C, the only product not seen from ABS polymer was 2,4-di-tert-butyl-phenol. ABS-CNT released emissions of all 11 major products. At 230°C, there were no detections of α -methylstyrene or 2,4-di-tert-butylphenol from ABS, and no benzaldehyde detections in any samples.

For the 1-minute reaction time samples, the analysis of multiple samples in series greatly increased the number of compounds detected at 230°C compared to the 100 mg pyrolysis samples. Benzaldehyde, α -methylstyrene, and acetophenone were not detected in either polymer matrix, and 2-phenyl-2-propanol, was only seen in ABS, and 2,4-di-tertbutylphenol was only seen in ABS-CNT. All other products were detected in both filaments. At 300°C, benzaldehyde was still non-detect for all samples, and 2,4-di-tertbutylphenol was again not detected for ABS.

Full tables of emission rates for all major products and samples, for both pyrolysis and oxidative pyrolysis, are available in Appendix A.

Table 4.2. Major products only detected in oxidative pyrolysis, their proposed source, and their chemical structure.

Compound	Source	Structure
Benzaldehyde	Oxidation of backbone cleavage intermediate	
2,6-di-tert-butylquinone	Oxidation of 2,4-di-tert-butylphenol	

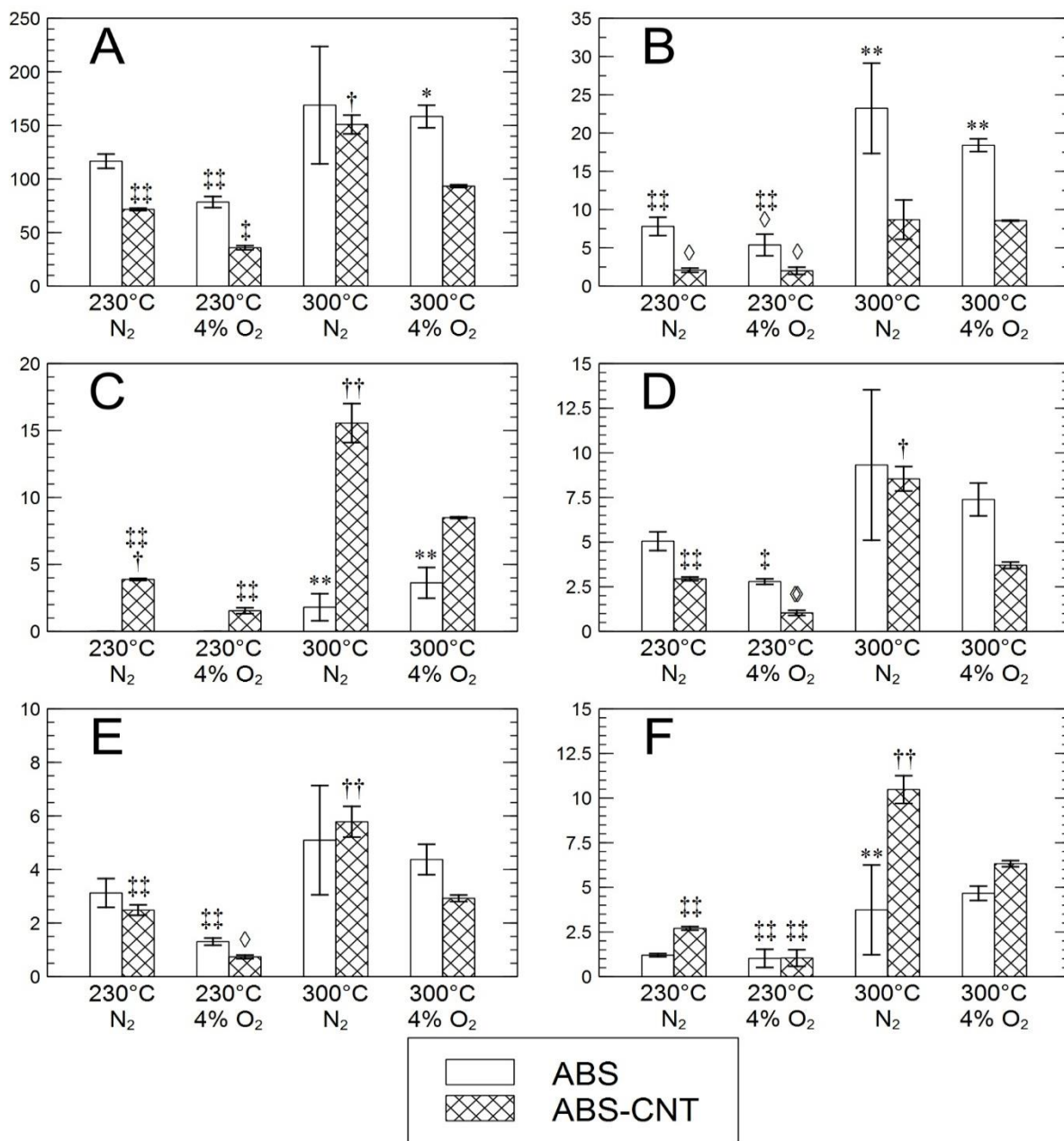
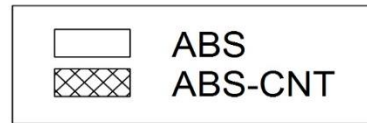
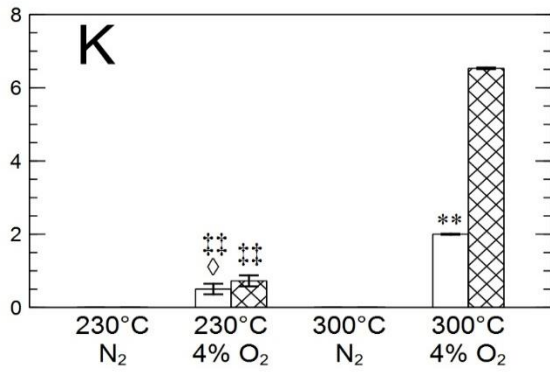
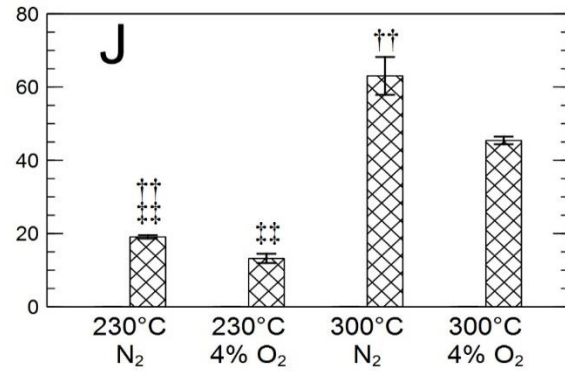
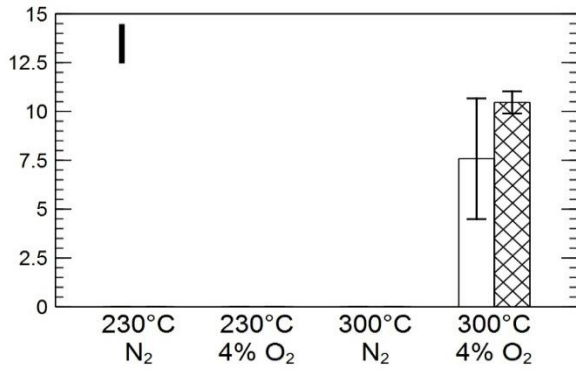
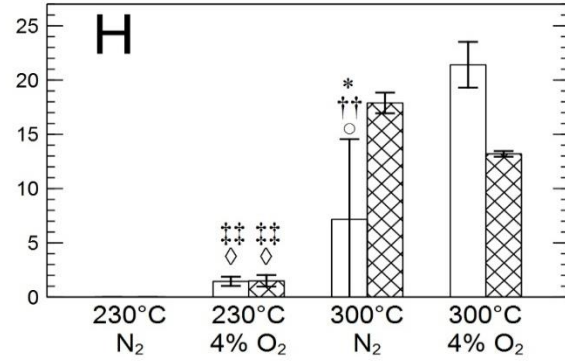
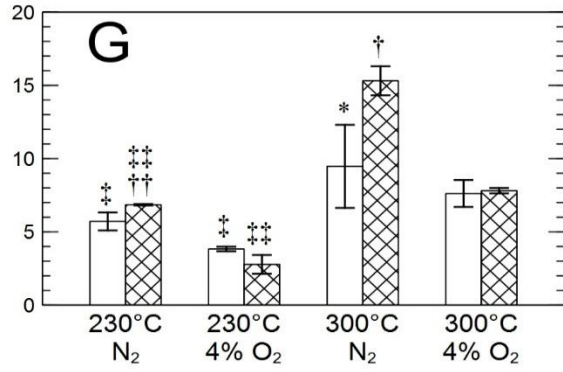


Figure 4.3. Summary of VOC emissions (µg/g) from ABS and ABS-CNT filament by temperature and oxygen content. A = styrene, B = 2-phenyl-2-propanol, C = α-methylstyrene, D = 4-vinylcyclohexene, E = isopropylbenzene, F = TMSN, G = ethylbenzene, H = acetophenone, I = benzaldehyde, J = 2,4-di-tert-butylphenol, K = 2,6-di-tert-butylquinone. Statistical significance determined using ANOVA with a post-hoc Tukey test. ‡ = statistical significance between 230 and 300°C, † = statistical significance between O₂ and N₂, * = statistical significance between ABS and ABS-CNT, and ◇ = below calculated MDL. Single symbol represents p-value < 0.05, double symbol represents p-value < 0.01. ○ = Value equals one detection averaged with two 0.5*MDLs (figure cont'd)



5. Discussion

5.1. Mass Optimization

The shapes of the mass versus response plots in Figure 4.1 resemble an exponential curve at 200°C, a linear curve at 230°C, and a logarithmic curve at 300°C. The relationship seen at 300°C suggests that surface area may have had a greater effect on the amount of volatiles released compared to mass. When the samples were heated, they often partially melted and expanded to fill more of the diameter of the basket. This limited the amount of surface area in contact with the carrier gas, and therefore reduced the emissions from the sample. This does not have as much of an effect at the lower temperatures, as the sample does not melt as much. In addition, surface area to volume ratio decreases with increasing volume, meaning that each increase in mass should have a smaller increase in emissions.

5.2. Degradation Mechanism

Figure 5.1 presents the proposed degradation pathway of ABS polymer. Three paths are presented based on the cleavage of bonds to β -carbons relative to styrene and acrylonitrile moieties. Path A shows cleavage which releases an isopropyl benzene molecule with an unpaired electron. This can either abstract a hydrogen from another source and remain isopropyl benzene, lose another hydrogen and form α -methylstyrene, or react with oxygen, water, or a hydroxyl radical to form 2-phenyl-2-propanol. Path B occurs when an ethylbenzene radical is cut from the chain. Through similar reactions as described for Path A, this can form ethylbenzene, styrene, acetophenone, or benzaldehyde. Path C involves the emission of butadiene monomers which then dimerize to form 4-vinylcyclohexene. TMSN is a byproduct of the

polymerization process⁷⁸ and 2,4-di-tert-butylphenol is involved in UV-stabilization⁷⁹. These are likely encased within the polymer matrix and released upon heating. 2,6-di-tert-butylquinone is an oxidation product of 2,4-di-tert-butylphenol or other similar UV-stabilizers.

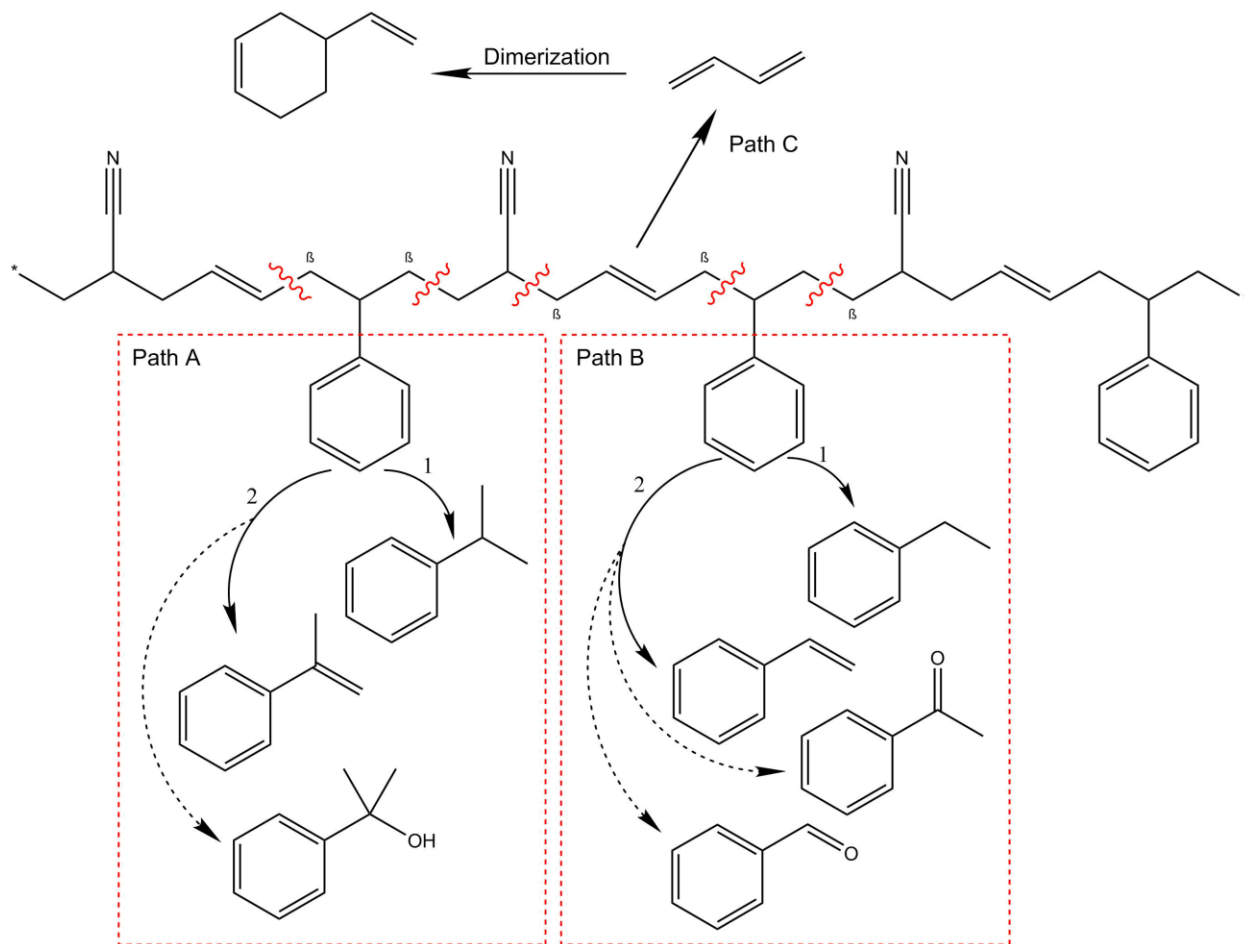


Figure 5.1. Proposed thermal degradation pathway of ABS polymer.

5.3. Effect of Carbon Nanotubes

The ratios of products within these pathways were influenced by the presence of both carbon nanotubes and gas phase oxygen. The inclusion of carbon nanotubes into ABS filament changed both the total VOC emissions and the emission profile. With the exception of pyrolysis at 300°C, the CNT containing samples produced less VOCs in

total compared to pure ABS. This decrease is primarily due to the reduction in emissions of styrene. There was also a shift in the distribution of products within Path A. α -methylstyrene emissions significantly increased (Figure 4.3C) and 2-phenyl-2-propanol emissions (Figure 4.3B) significantly decreased (isopropylbenzene remained largely unaffected). This occurred both under pyrolytic and oxidative conditions, which provides evidence that this pathway is unaffected by the presence of gas phase oxygen, and instead, the formation of 2-phenyl-2-propanol is dependent upon oxygen adsorbed to the polymer matrix. It has been proposed that molecular oxygen can adsorb to carbon nanotubes^{80,81}, which could then decrease the concentration available for reaction with the isopropyl benzene radical.

The presence of nanotubes did not, however, seem to affect the preference for Path A or Path B products. As shown in Figure 5.2., after styrene is removed from the calculations, there is little difference between the total emissions of Path A and B, both within samples and between ABS and ABS-CNT samples. This also demonstrates that the majority of styrene emissions are likely due to unreacted monomer release instead of backbone cleavage. The decrease of these styrene emissions seen in most CNT samples is likely a result of unreacted styrene monomers being adsorbed to the nanotubes in the matrix, and therefore less likely to volatilize when heated. This affinity of VOCs for carbon nanotubes⁸² could also be contributing to the decreased yields of 2-phenyl-2-propanol, isopropyl benzene (not significant), and 4-vinylcyclohexene (not significant) in CNT containing samples. In addition, carbon nanotubes have been demonstrated to scavenge free radicals⁸³⁻⁸⁵, which could also account for some of

these decreased yields. However, this should lead to a decrease in all products of polymer decomposition, which is not shown by the data.

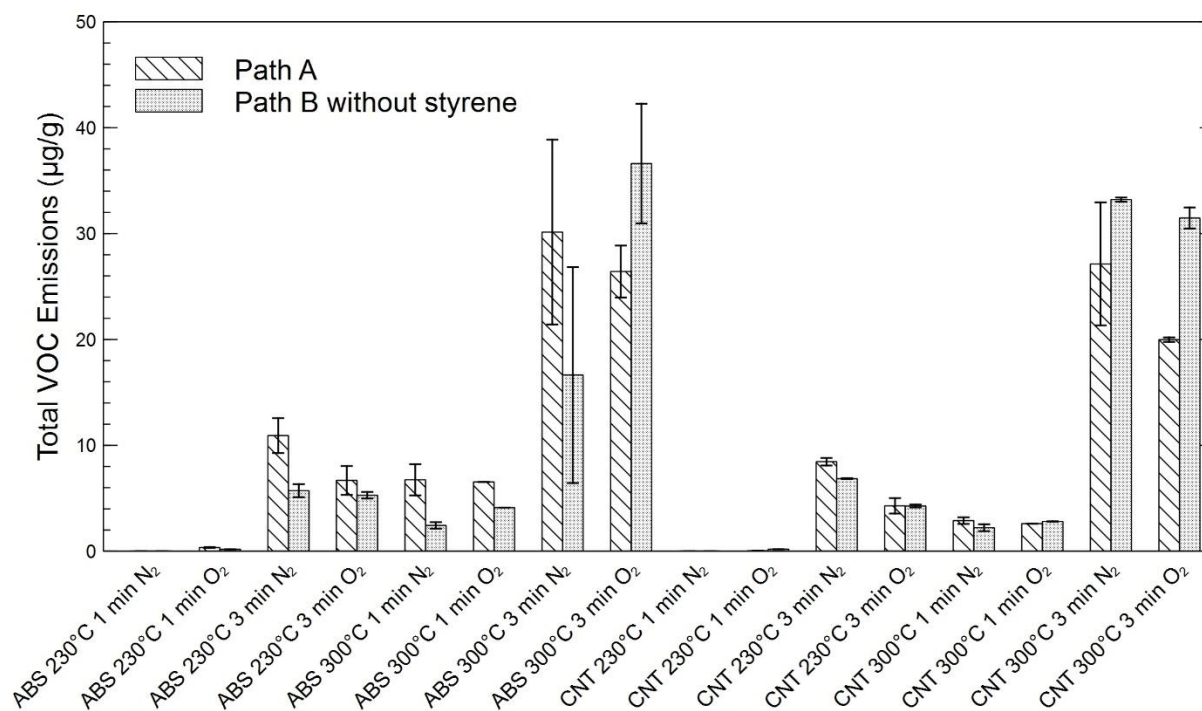


Figure 5.2. Total VOC emissions from products in Path A and Path B of the degradation scheme, without styrene, separated by reaction parameters.

It is unclear as to why 2,4-di-tert-butylphenol was only detected in emissions from CNT containing ABS filament, or why TMSN and 2,6-di-tert-butylquinone were detected in significantly higher amounts. These are products related to the synthesis of the polymer and its UV stability, which could mean that the inclusion of CNTs requires a different method of synthesis and/or amount of these products. Another possibility is that the nanotubes are somehow triggering the release of these compounds, through an unknown mechanism.

5.4. Effect of Oxygen

The effect of oxygen on emissions seems to be a bit simpler. There was a general trend of decreased emissions (some significant and some not) for compounds that do not contain oxygen in their formula, while acetophenone generally increased, and 2,6-di-tert-butylquinone and benzaldehyde were detected as new major products. The decrease can be explained by increased formation of oxidized products such as acetophenone and benzaldehyde, and/or oxidation of products to low molecular weight compounds including CO and CO₂ (which were not analyzed in this study). A study by Hoff et al. showed a similar relationship between ABS thermal degradation in nitrogen and in air, with the air exposed samples showing higher emissions of acetophenone and benzaldehyde, as well as small molecular weight alcohols and aldehydes¹⁶. Stefaniak also reports acetaldehyde, ethanol, acetonitrile, acetone, and isopropyl alcohol with higher emission rates from a 3D printer than any other product besides styrene³. Another possibility is described by Erickson and Oelfke⁸⁶, which involves dilute concentrations of oxygen present during thermal decomposition of polymers forming more thermally stable intermediates, slowing down the decomposition process. TMSN and 2,4-di-tert-butylphenol also decreased, though the mechanism for this is unclear.

5.5. Exposure Assessment

Although this study did not capture emissions directly from the use of a 3D printer, the results are still relevant to that scenario and can be used to model an exposure. Styrene had by far the highest measured emission rate, and also has the most well-established toxicological data, making it the model compound for this scenario. As pure ABS polymer showed higher emissions of styrene compared to the

CNT containing filament, and it is the more commonly used formulation, the exposure calculated below is based off of values obtained from non-CNT containing samples.

The highest styrene emission rate measured was 170 $\mu\text{g/g}$, however this comes from a 3-minute heating time at 300°C in pure nitrogen, which is not the most relevant to a typical home-use scenario. A more appropriate value for the estimated styrene emission rate from a 3D printer may be the 5.32 $\mu\text{g/g}$ measured for ABS in a 1-minute reaction at 230°C under 4% O_2 conditions. In studies measuring 3D printer emissions from ABS by Steinle and Floyd^{4,5}, the amount of VOCs emitted per minute was roughly one tenth of the emissions per gram printed, due to printing speeds close to 0.1 g/min. Applying this printing speed to the emission rate from this study gives gives 0.532 $\mu\text{g/min}$. This number is an order of magnitude lower than the 4.8 $\mu\text{g/min}$ and 5.8 $\mu\text{g/min}$ values reported by Floyd and Steinle for styrene^{4,5}. However, the measured value for styrene emissions from ABS at 230°C under 4% O_2 for 3 minutes was 78.5 $\mu\text{g/g}$, which is close to the value of 58 $\mu\text{g/g}$ reported by Steinle⁴ and gives 7.85 $\mu\text{g/min}$ when multiplied by the printing speed.

These two values are simply approximations, as heating in the STDS is not the same as heating in a 3D printer. In a 3D printer, the amount of time a section of filament resides in the hot zone is dependent on the printing speed and the length of zone. In the STDS, a single 50 mg piece was heated for 1 or 3 minutes to account for this, but may not match up well with the heating times experienced in either Steinle or Floyd. The extruder temperature, printing time, and the specific filaments used are also important factors in the quantity of emissions generated and likely have an effect as well. Exposure estimations are calculated below for both estimated values.

Let it be assumed that a 3D printer is located in a small unventilated room of approximately 40 m³ volume and constantly printing, as shown in Figure 5.3. Based on the 0.532 µg/min styrene emission rate, it would take approximately 5,000 to reach the acute exposure guideline level of 20 ppm (Table 2.2). For chronic exposure, the EPA RfC is 1 mg/m³ (Table 2.3), and it would take 52 days of printing to reach this level.

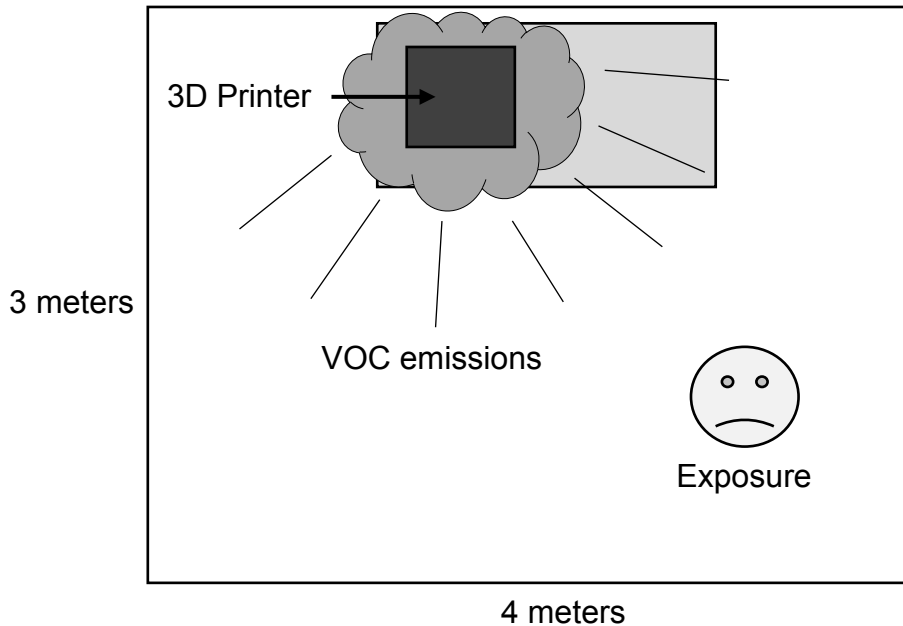


Figure 5.3. Diagram of exposure scenario involving 3D printing in a small room.

Performing the same calculations for the 7.85 µg/min emission rate leads to around 325 days of printing to reach the acute exposure guideline level, but only 3.5 days to reach the chronic RfC. Based on these numbers alone, it is likely that very little acute risk from styrene exposure is associated with using a single 3D printer with ABS filament, though there may be potential for chronic health effects.

Of course, there are many assumptions involved in this scenario. The actual exposure would likely be lower due to the fact that most rooms are at least somewhat ventilated, a printer is not likely running constantly for days or weeks at a time, and this

ignores adsorption of contaminants onto surfaces in the room. On the other hand, this estimate is only for styrene, ignoring the emissions of other compounds which may have additive or even synergistic toxic effects, the extrusion temperature may be set higher than the 230°C used in this example, leading to overall higher emissions, the distribution of VOCs will not be uniform throughout the room during printing, with greater concentrations closer to the printer, and there may be more than one printer operating in the same room. Additionally, these regulatory values are based on non-cancer effects, while styrene has also been classified as probably carcinogenic to humans and a few other products are listed as possibly carcinogenic.

6. Conclusion

This study qualitatively and quantitatively assessed the formation of VOCs during thermal decomposition of ABS 3D printer filament and how it is affected by temperature, heating time, the presence of oxygen, and the inclusion of carbon nanotubes in the polymer matrix. Analysis was carried out using a modified system for thermal diagnostic studies with a vertical reactor and a GC-MS. The major product detected in all reactions was styrene, with an emission rate ranging from 5.32 $\mu\text{g/g}$ to approximately 170 $\mu\text{g/g}$ at the highest temperature, longest reaction time, and no oxygen present.

Increased temperature and increased heating time had the expected effects of increasing emissions from all measured products. There was no significant change in the distribution of products due to either parameter.

Presence of oxygen in the reaction gas increased the emissions of oxidized products such as benzaldehyde and acetophenone, while 2-phenyl-2-propanol was not significantly affected. This evidences the fact that different pathways of ABS thermal decomposition prefer different sources of oxygen, with one seemingly depending on oxygen adsorbed to the polymer matrix and the other more dependent on the presence of gas phase oxygen. Non-oxygenated products decreased in abundance with the addition of oxygen, likely due to the increase of oxygenated products, both identified and non-identified, and possibly the creation of stable oxygenated intermediates.

Carbon nanotubes had the apparent effect of decreasing the available adsorbed oxygen in the matrix. Yields of 2-phenyl-2-propanol decreased, while there were increased emissions of α -methylstyrene, another product in the same proposed degradation pathway. In addition, many VOCs have been shown to have an affinity for

carbon nanotubes, which may explain the decrease in styrene emissions also seen in the CNT containing samples. Overall VOC emissions from Path A and Path B were generally very similar across samples once styrene was not counted, leading to the conclusion that the majority of styrene emissions are from trapped monomers, rather than backbone cleavage.

There are many assumptions to be made when applying the results of this work to an exposure scenario relevant for home 3D printing. With that in mind, a model exposure scenario showed that there is likely insufficient styrene emitted from printing using ABS filament and tested printing conditions to pose a non-cancer human health risk outside of any extreme-use scenarios. Styrene has only been recently classified as a probable human carcinogen, and a reference value for risk calculations is not yet available. Compounds other than styrene are emitted in lower amounts, yet may still pose a health risk. There is the possibility for additive or even synergistic effects in the mixture of emitted VOCs, some of which also lack a significant amount of toxicological data. Different formulations of ABS polymer may also exhibit different levels and relative amounts of these decomposition products.

This study demonstrated the efficacy of the modified STDS in measuring toxic VOC emissions from 3D printer filaments. A future direction for this work includes improving the method to be able to detect smaller molecular weight products. This would allow for a better overall emission profile to be developed and studied under changing parameters. In addition, the toxic compounds hydrogen cyanide and 1,3-butadiene fall into this category and have been previously detected as thermal decomposition products of ABS polymer. Once the method has been improved,

studying the effects of different filament additives on emissions is the next direction for this work.

Appendix A. Tables of Emission Rates

Table A.1. Emission rates in µg/g for 1-minute reaction time samples

	Emission Rates (µg/g) for 1-Minute Reactions									
	200°C		230°C				300°C			
	N ₂		N ₂		4% O ₂		N ₂		4% O ₂	
	ABS	ABS-CNT	ABS	ABS-CNT	ABS	ABS-CNT	ABS	ABS-CNT	ABS	ABS-CNT
α-Methylstyrene	--	--	--	--	--	--	--	1.0	1.0	1.1
2,4-Di-tert-butylphenol*	--	0.6	--	1.2	0.1 ◇	2.5	--	6.8	--	1.4
2,6-Di-tert-butylquinone*	--	--	--	--	0.05	0.2	--	--	0.8	0.4
2-Phenyl-2-propanol	--	--	--	--	0.3 ◇	--	5.2	0.7 ◇	4.7	1.1 ◇
Acetophenone	--	--	--	--	--	--	--	--	2.5	1.0 ◇
Benzaldehyde	--	--	--	--	--	--	--	--	--	--
Cyclohexene, 4-ethenyl-	--	--	--	--	0.2 ◇	0.1 ◇	2.2	0.8	1.6	0.6
Ethylbenzene	--	--	--	--	0.2 ◇	0.2 ◇	2.4	1.8	1.6	1.8
Isopropylbenzene	--	--	--	--	0.1 ◇	0.1 ◇	1.6	0.6 ◇	0.9	0.4
Styrene	3.3	1.1 ◇	10.5	2.7	5.3	2.1	49.5	20.6	40.0	19.1
Tetramethylsuccinonitrile	--	--	--	--	0.1 ◇	0.1 ◇	0.6	0.7	0.9	0.8
Total	3.6	1.9	10.5	3.8	6.3	5.2	61.4	33.1	53.9	27.7

-- = Non-detect; ◇ = Below calculated MDL; * = using calibration curve for 2,6-di-tert-butylphenol;

Table A.2. Emission rates in µg/g for 3-minute reaction time samples

	Emission Rates (µg/g) for 3-Minute Reactions									
	200°C		230°C				300°C			
	N ₂		N ₂		4% O ₂		N ₂		4% O ₂	
	ABS	ABS-CNT	ABS	ABS-CNT	ABS	ABS-CNT	ABS	ABS-CNT	ABS	ABS-CNT
α-Methylstyrene	--	1.7	--	3.9	--	1.5	1.8	15.6	3.6	8.5
2,4-Di-tert-butylphenol*	--	7.9	--	19.1	--	13.2	--	63.0	--	45.4
2,6-Di-tert-butylquinone*	--	--	--	--	0.5	0.7	--	--	2.0	6.5
2-Phenyl-2-propanol	3.2 ◇	--	7.8	2.1 ◇	5.4 ◇	2.0 ◇	23.2	8.7	18.4	8.6
Acetophenone	--	--	--	--	1.4 ◇	1.5 ◇	7.2**	17.9	21.4	13.2
Benzaldehyde	--	--	--	--	--	--	--	--	7.6	10.5
Cyclohexene, 4-ethenyl-	2.4	1.3	5.1	2.9	2.8	1.0 ◇	9.3	8.5	7.4	3.7
Ethylbenzene	2.7	3.0	5.7	6.9	3.8	2.8	9.5	15.3	7.6	7.8
Isopropylbenzene	1.4	1.1 ◇	3.1	2.5	1.3	0.7 ◇	5.1	5.8	4.4	2.9
Styrene	63.2	35.4	116.6	71.7	78.5	35.8	168.9	150.9	158.4	93.3
Tetramethylsuccinonitrile	--	0.9	1.2	2.7	1.0	1.0	3.7	10.5	4.7	6.3
Total	72.8	51.4	139.5	111.7	94.8	60.4	226.8	296.2	235.4	206.7

-- = Non-detect; ◇ = Below calculated MDL; * = using calibration curve for 2,6-di-tert-butylphenol;

** = Only detected in 1 of 3 runs. Reported value represents average of detected concentration and two 0.5*MDL values

Appendix B. Example Chromatograms

Figure B.1. Chromatogram for 230°C, 1-minute, ABS, 4% O₂ sample

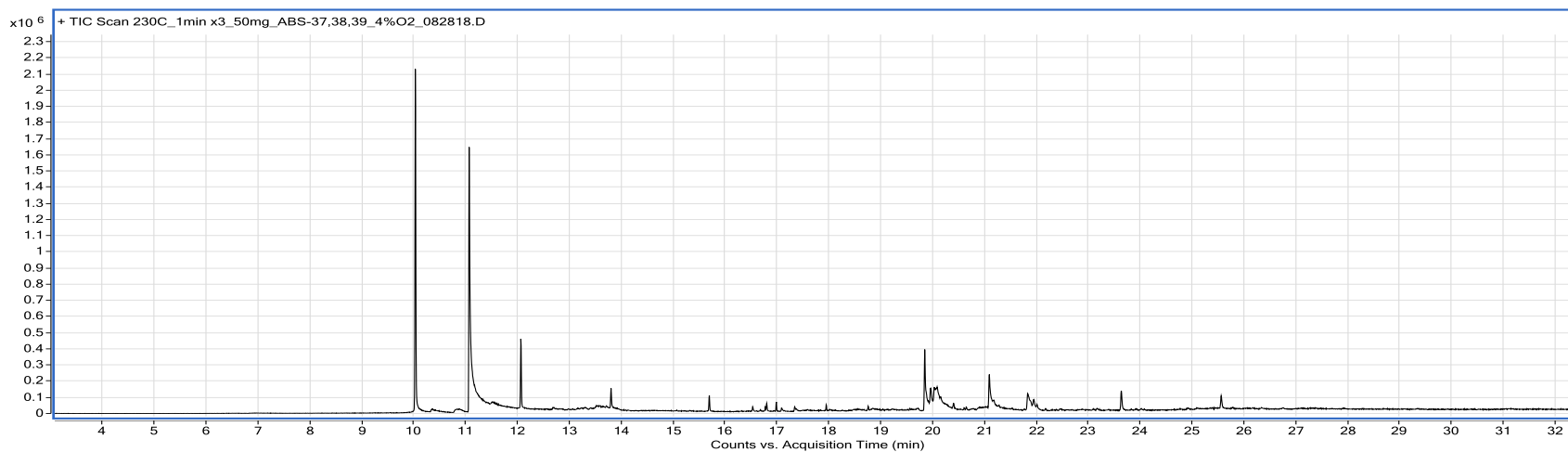


Figure B.2. Chromatogram for 230°C, 1-minute, ABS-CNT, 4% O₂ sample

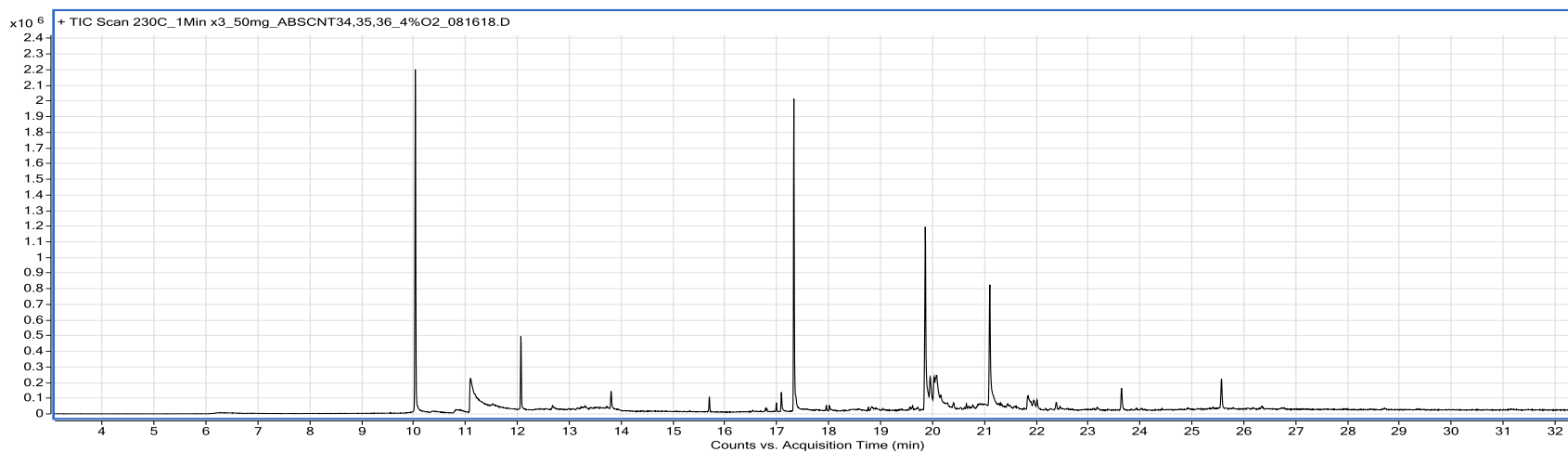


Figure B.3. Chromatogram for 230°C, 3-minute, ABS, 4% O₂ sample

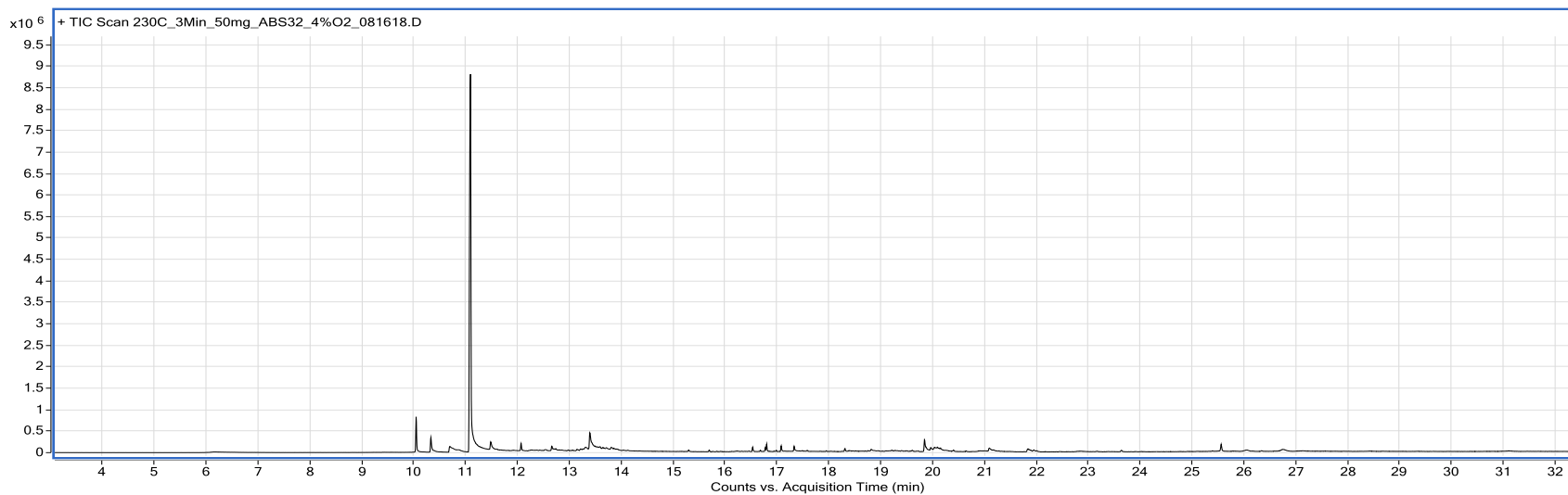


Figure B.4. Chromatogram for 230°C, 3-minute, ABS-CNT, 4% O₂ sample

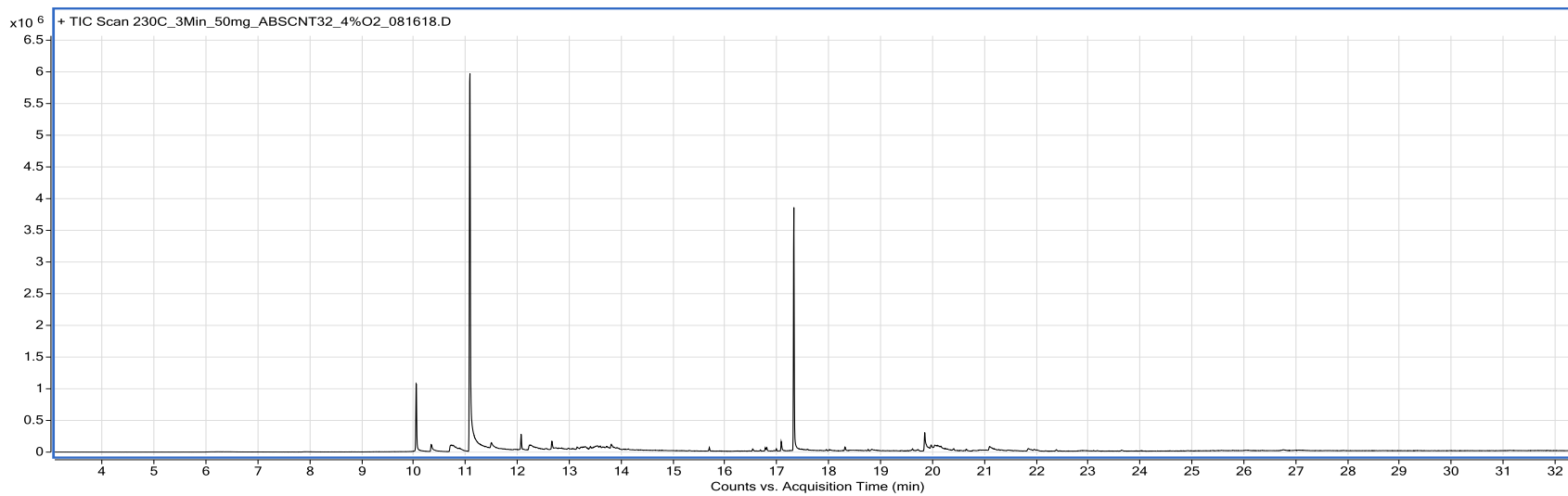


Figure B.5. Chromatogram for 300°C, 1-minute, ABS, 4% O₂ sample

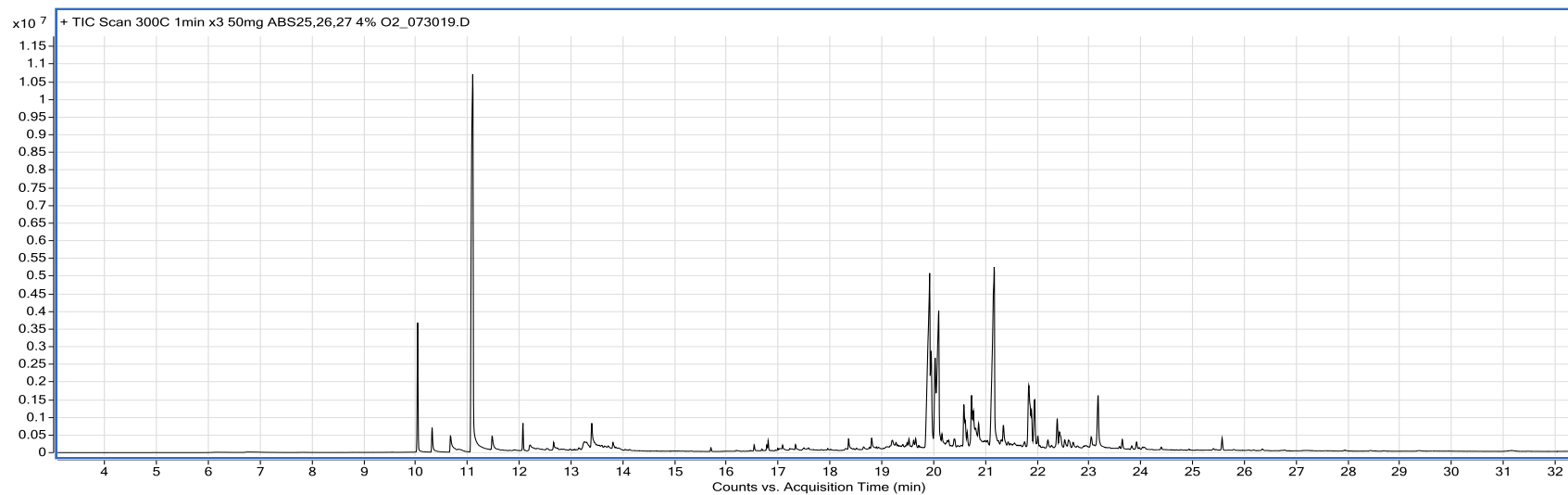


Figure B.6. Chromatogram for 300°C, 1-minute, ABS-CNT, 4% O₂ sample

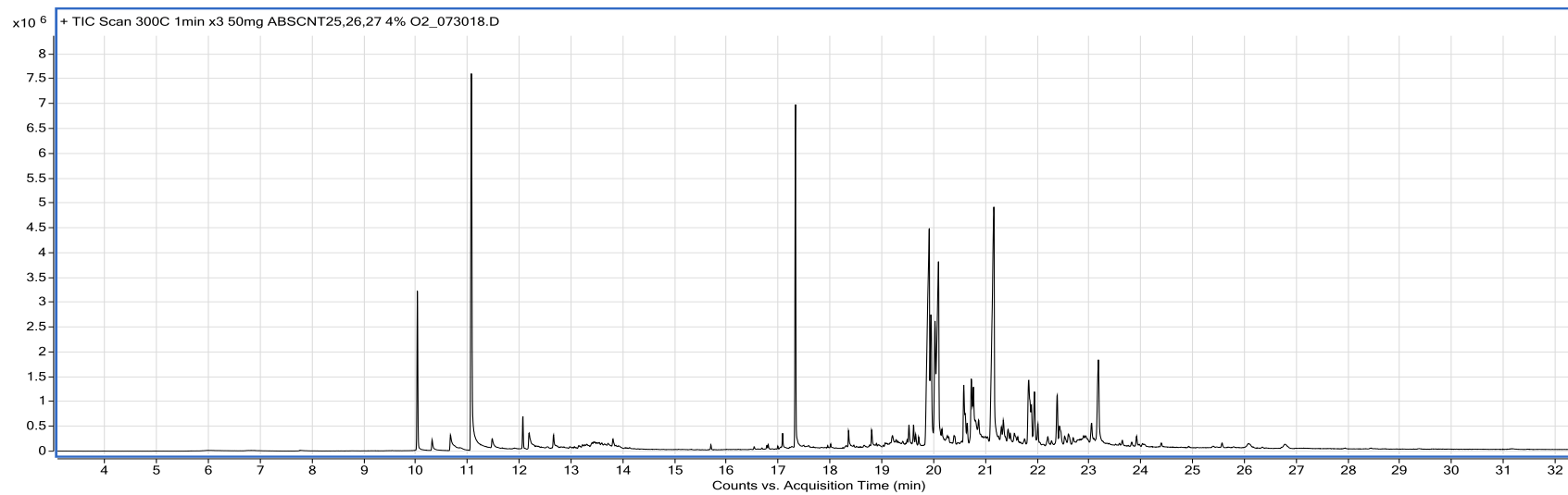


Figure B.7. Chromatogram for 300°C, 3-minute, ABS, 4% O₂ sample

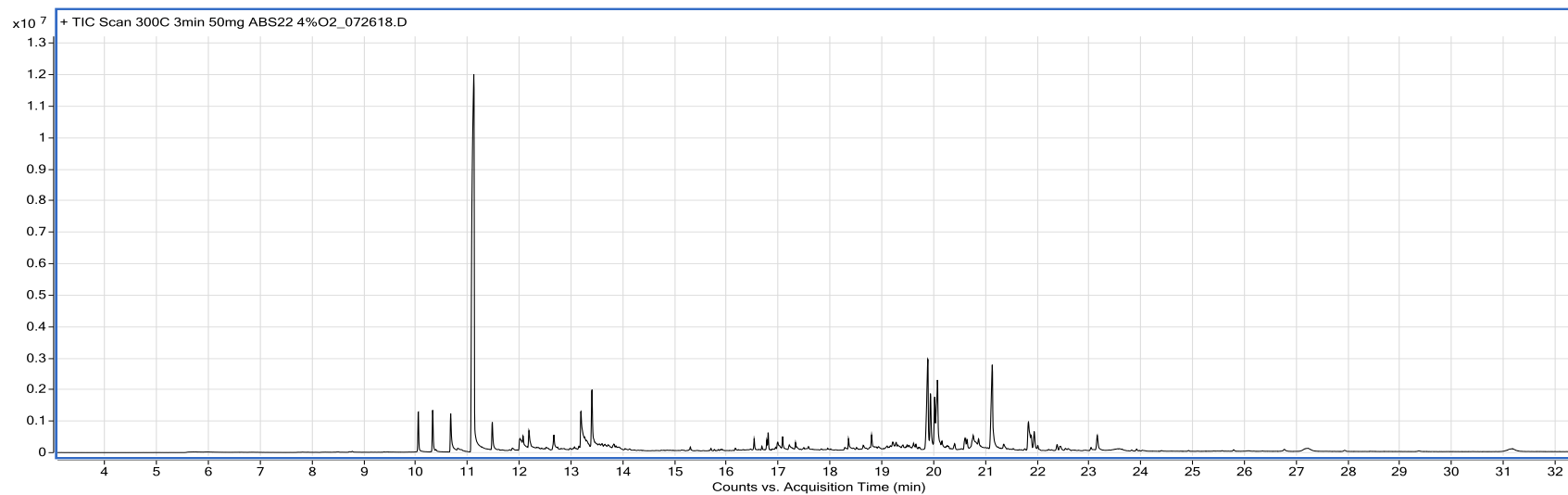


Figure B.8. Chromatogram for 300°C, 3-minute, ABS-CNT, 4% O₂ sample

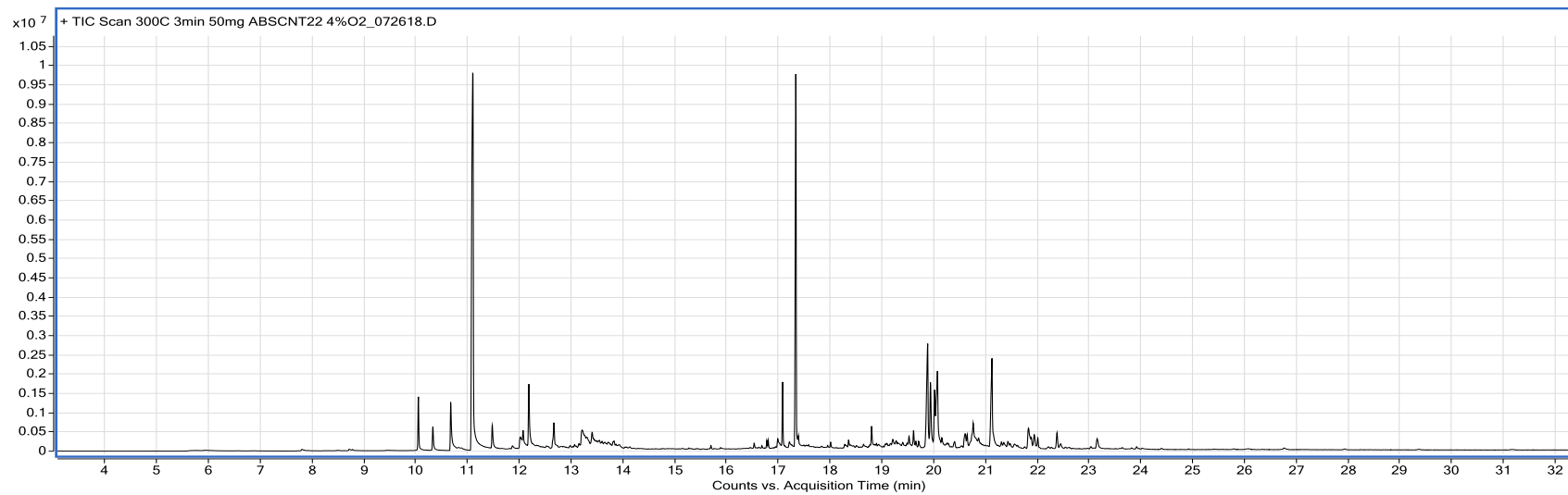


Figure B.9. Chromatogram for standard curve sample with 800 and 1,600 $\mu\text{g}/\text{mL}$ concentrations

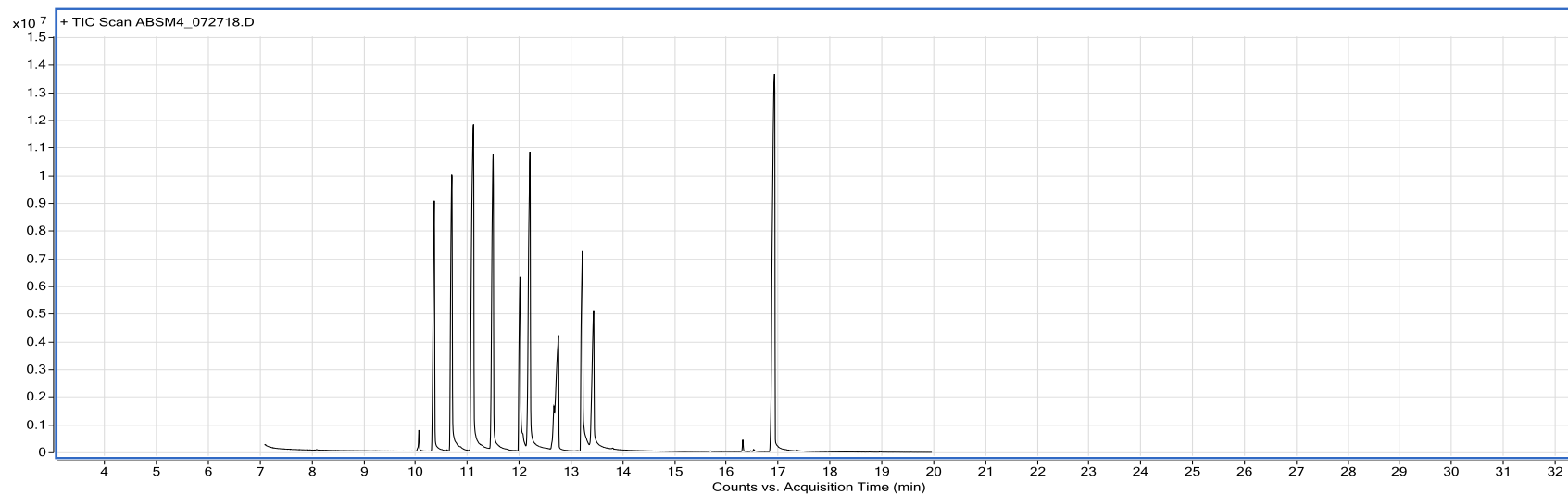
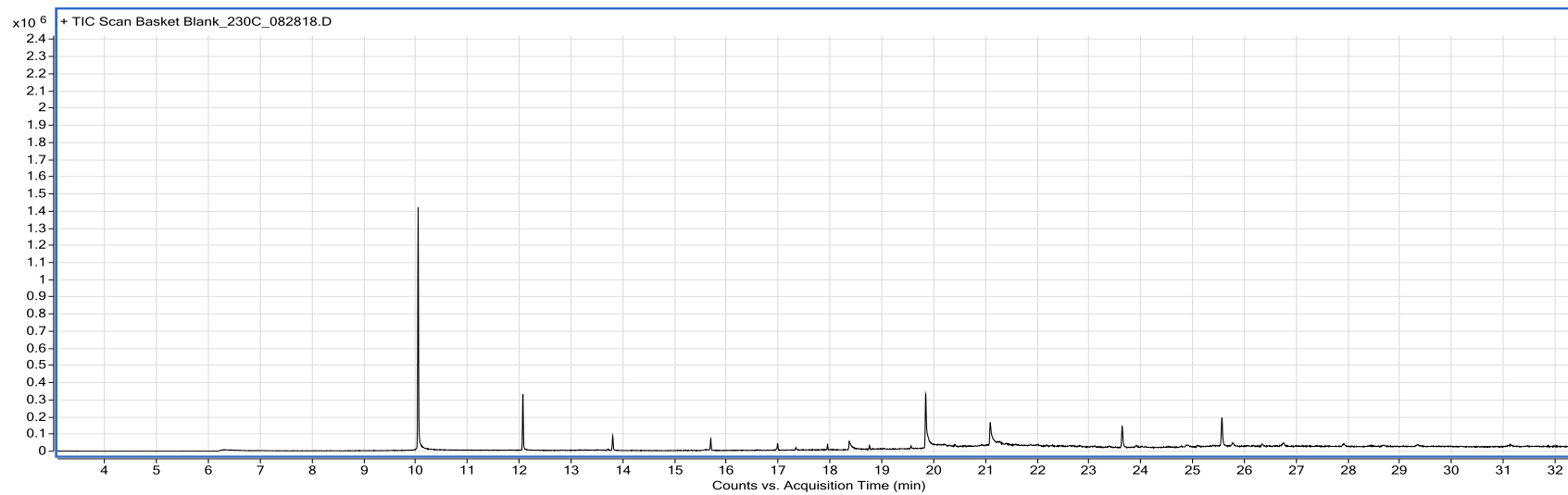


Figure B.10. Chromatogram for basket blank sample



Appendix C. Permissions

Dean Lay
Louisiana State University
Department of Environmental Sciences

January 28, 2019

Dr. Souhail R. Al-Abed, and Dr. Phillip Potter
US EPA
Cincinnati, OH, 45220

Dear Dr. Al-Abed and Dr. Potter:

I am completing a Master's thesis at Louisiana State University entitled "VOC Emission Factors from 3D Printers – ABS (Acrylonitrile-Butadiene-Styrene) Type Filaments." I would like your permission to print the following material in my thesis:

The data and ideas presented in our co-authored paper, "VOC Emissions and Formation Mechanisms from Carbon Nanotube Composites During 3D Printing" (working title). Figures and language of the text have been altered from what appears in the paper, however the data and overall ideas remain largely unchanged.

The requested permission extends to any future revisions and editions of my thesis, including non-exclusive world rights in all languages. These rights will in no way restrict republication of the material in any other form by you or by others authorized by you.

To grant this permission, please sign where indicated below and return this letter to me. Please contact me should you have any questions or need additional information. Thank you very much.

Sincerely,

PERMISSION GRANTED FOR THE USE REQUESTED ABOVE:

Phillip Potter

Printed name



Signature

Date: 2/5/19

References

1. Stephens, B., Azimi, P., El Orch, Z. & Ramos, T. Ultrafine particle emissions from desktop 3D printers. *Atmos. Environ.* **79**, 334–339 (2013).
2. Yi, J. *et al.* Emission of particulate matter from a desktop three-dimensional (3D) printer. *J. Toxicol. Environ. Heal. Part A* **79**, 453–465 (2016).
3. Stefaniak, A. B. *et al.* Characterization of chemical contaminants generated by a desktop fused deposition modeling 3-dimensional Printer. *J. Occup. Environ. Hyg.* **14**, 540–550 (2017).
4. Steinle, P. Characterization of emissions from a desktop 3D printer and indoor air measurements in office settings. *J. Occup. Environ. Hyg.* **13**, 121–132 (2016).
5. Floyd, E. L., Wang, J. & Regens, J. L. Fume emissions from a low-cost 3-D printer with various filaments. *J. Occup. Environ. Hyg.* **14**, 523–533 (2017).
6. United States Environmental Protection Agency. Volatile Organic Compounds' Impact on Indoor Air Quality. (2017). Available at: <https://www.epa.gov/indoor-air-quality-iaq/volatile-organic-compounds-impact-indoor-air-quality>. (Accessed: 2nd October 2018)
7. International Agency for Research on Cancer. Agents Classified by the IARC Monographs, Volumes 1-123. (2018).
8. Mendell, M. J. Indoor residential chemical emissions as risk factors for respiratory and allergic effects in children: A review. *Indoor Air* (2007). doi:10.1111/j.1600-0668.2007.00478.x
9. Wolkoff, P., Wilkins, C. K., Clausen, P. A. & Nielsen, G. D. Organic compounds in office environments - Sensory irritation, odor, measurements and the role of reactive chemistry. *Indoor Air* (2006). doi:10.1111/j.1600-0668.2005.00393.x
10. United States Environmental Protection Agency. Introduction to Indoor Air Quality. (2018). Available at: <https://www.epa.gov/indoor-air-quality-iaq/introduction-indoor-air-quality>. (Accessed: 12th March 2018)
11. Zhang, J. & Smith, K. R. Indoor air pollution: A global health concern. *British Medical Bulletin* (2003). doi:10.1093/bmb/ldg029
12. Lucattini, L. *et al.* A review of semi-volatile organic compounds (SVOCs) in the indoor environment: occurrence in consumer products, indoor air and dust. *Chemosphere* (2018). doi:10.1016/j.chemosphere.2018.02.161

13. Tichenor, B. A. & Mason, M. A. Organic emissions from consumer products and building materials to the indoor environment. *J. Air Pollut. Control Assoc.* (1988). doi:10.1080/08940630.1988.10466376
14. Contos, D. A. *et al.* Sampling and Analysis of Volatile Organic Compounds Evolved During Thermal Processing of Acrylonitrile Butadiene Styrene Composite Resins. *J. Air Waste Manage. Assoc.* **45**, 686–694 (1995).
15. Rutkowski, J. V & Levin, B. C. Acrylonitrile-butadiene-styrene copolymers (ABS): Pyrolysis and combustion products and their toxicity? a review of the literature. *Fire Mater.* **10**, 93–105 (1986).
16. Hoff, A., Jacobsson, S. & Pfaffli, P. Degradation products of plastics. Polyethylene and styrene-containing thermoplastics - Analytical, occupational and toxicologic aspects. *Scand. J. Work. Environ. Heal.* (1982). doi:2505 [pii]
17. Wang, X., Jiang, M., Zhou, Z., Gou, J. & Hui, D. 3D printing of polymer matrix composites: A review and prospective. *Compos. Part B Eng.* **110**, 442–458 (2017).
18. Crump, S. *United States Patent 5,121,329: Apparatus and method for creating three-dimensional objects.* (1992).
19. Olivera, S., Muralidhara, H. B., Venkatesh, K., Gopalakrishna, K. & Vivek, C. S. Plating on acrylonitrile–butadiene–styrene (ABS) plastic: a review. *Journal of Materials Science* (2016). doi:10.1007/s10853-015-9668-7
20. Massey, L. K. Acrylonitrile-Butadiene-Styrene (ABS). in *The Effect of Sterilization Methods on Plastics and Elastomers* **1**, 19–38 (Elsevier, 2005).
21. Czégény, Z., Jakab, E., Blazsó, M., Bhaskar, T. & Sakata, Y. Thermal decomposition of polymer mixtures of PVC, PET and ABS containing brominated flame retardant: Formation of chlorinated and brominated organic compounds. *J. Anal. Appl. Pyrolysis* **96**, 69–77 (2012).
22. Ghoshal, S. Polymer/Carbon Nanotubes (CNT) Nanocomposites Processing Using Additive Manufacturing (Three-Dimensional Printing) Technique: An Overview. *Fibers* **5**, 40 (2017).
23. Filaments Production and Fused Deposition Modelling of ABS/Carbon Nanotubes Composites. *Nanomaterials* **8**, 49 (2018).
24. Conner, B. P. *et al.* Making sense of 3-D printing: Creating a map of additive manufacturing products and services. *Addit. Manuf.* **1–4**, 64–76 (2014).
25. Çetinkaya, O., Demirci, G. & Mergo, P. Effect of the different chain transfer agents on molecular weight and optical properties of poly(methyl methacrylate). *Opt. Mater. (Amst).* **70**, 25–30 (2017).

26. Mayo, F. R. *Chain Transfer in the Polymerization of Styrene: The Reaction of Solvents with Free Radicals*. (1943).
27. Chemistry LibreTexts. Free Radical Polymerization. (2015). Available at: [https://chem.libretexts.org/LibreTexts/Purdue/Purdue_Chem_26100%3A_Organic_Chemistry_I_\(Wenthold\)/Chapter_08%3A_Reactions_of_Alkenes/8.7.%09Polymerization/Free_Radical_Polymerization](https://chem.libretexts.org/LibreTexts/Purdue/Purdue_Chem_26100%3A_Organic_Chemistry_I_(Wenthold)/Chapter_08%3A_Reactions_of_Alkenes/8.7.%09Polymerization/Free_Radical_Polymerization). (Accessed: 11th January 2018)
28. Dresselhaus, M. S. & Avouris, P. Introduction to Carbon Materials Research. in *Carbon Nanotubes: Synthesis, Structure, Properties, and Applications* (eds. Dresselhaus, M. S., Dresselhaus, G. & Avouris, P.) 1–9 (Springer Berlin Heidelberg, 2001). doi:10.1007/3-540-39947-X_1
29. Charlier, J.-C. & Iijima, S. Growth Mechanisms of Carbon Nanotubes. in *Carbon Nanotubes: Synthesis, Structure, Properties, and Applications* (eds. Dresselhaus, M. S., Dresselhaus, G. & Avouris, P.) 55–81 (Springer Berlin Heidelberg, 2001). doi:10.1007/3-540-39947-X_4
30. Dul, S., Fambri, L. & Pegoretti, A. Fused deposition modelling with ABS–graphene nanocomposites. *Compos. Part A Appl. Sci. Manuf.* **85**, 181–191 (2016).
31. Yang, S., Rafael Castilleja, J., Barrera, E. V. & Lozano, K. Thermal analysis of an acrylonitrile–butadiene–styrene/SWNT composite. *Polym. Degrad. Stab.* **83**, 383–388 (2004).
32. ASTM International. *Standard Terminology of Fire Standards*. (2018). doi:10.1520/E0176-18
33. Beyler, C. L. & Hirschler, M. M. Thermal Decomposition of Polymers. in *SFPE Handbook of Fire Protection Engineering 2* 111–131 (2002).
34. Streibel, T. *et al.* Evolved gas analysis (EGA) in TG and DSC with single photon ionisation mass spectrometry (SPI-MS): molecular organic signatures from pyrolysis of soft and hard wood, coal, crude oil and ABS polymer. *J. Therm. Anal. Calorim.* **96**, 795–804 (2009).
35. Hitachi High-Tech Science Corporation. *Thermal Decomposition Measurement of ABS resin I -Analysis by Quasi-Isothermal TG and TG/FT-IR Measurements*. (1995).
36. Herrera, M., Matuschek, G. & Kettrup, A. Fast identification of polymer additives by pyrolysis-gas chromatography/mass spectrometry. *J. Anal. Appl. Pyrolysis* **70**, 35–42 (2003).
37. Guillemot, M., Oury, B. & Melin, S. Identifying thermal breakdown products of thermoplastics. *J. Occup. Environ. Hyg.* **14**, 551–561 (2017).

38. National Library of Medicine (US). Acetophenone; Hazardous Substances Databank Number: 969. (2018). Available at: <http://toxnet.nlm.nih.gov/cgi-bin/sis/search2/r?dbs+hsdb:@term+@DOCNO+969>. (Accessed: 15th October 2018)
39. Jenner, P. M., Hagan, E. C., Taylor, J. M., Cook, E. L. & Fitzhugh, O. G. Food flavourings and compounds of related structure I. Acute oral toxicity. *Food Cosmet. Toxicol.* **2**, 327–343 (1964).
40. Final Report on the Safety Assessment of Benzaldehyde¹. *Int. J. Toxicol.* **25**, 11–27 (2006).
41. National Library of Medicine (US). Benzaldehyde; Hazardous Substances Databank Number: 388. (2016). Available at: <http://toxnet.nlm.nih.gov/cgi-bin/sis/search2/r?dbs+hsdb:@term+@DOCNO+388>. (Accessed: 4th December 2018)
42. Tabatabaie, T. & Floyd, R. A. Inactivation of glutathione peroxidase by benzaldehyde. *Toxicol. Appl. Pharmacol.* **141**, 389–393 (1996).
43. National Library of Medicine (US). Isopropylbenzene; Hazardous Substances Databank Number: 172. (2013). Available at: <http://toxnet.nlm.nih.gov/cgi-bin/sis/search2/r?dbs+hsdb:@term+@DOCNO+172>. (Accessed: 15th October 2018)
44. Tham, R. *et al.* Vestibulo-Ocular Disturbances in Rats Exposed to Organic Solvents. *Acta Pharmacol. Toxicol. (Copenh)*. **54**, 58–63 (1984).
45. Cushman, J. R., Norris, J. C., Dodd, D. E., Darmer, K. I. & Morris, C. R. Subchronic Inhalation Toxicity and Neurotoxicity Assessment of Cumene in Fischer 344 Rats. *Int. J. Toxicol.* **14**, 129–147 (1995).
46. National Library of Medicine (US). 2,4-di-tert-butylphenol; Hazardous Substances Databank Number: 8453. (2018). Available at: <http://toxnet.nlm.nih.gov/cgi-bin/sis/search2/r?dbs+hsdb:@term+@DOCNO+8453>. (Accessed: 4th December 2018)
47. Hirata-Koizumi, M. *et al.* Elevated susceptibility of newborn as compared with young rats to 2-tert-butylphenol and 2,4-di-tert-butylphenol toxicity. *Congenit. Anom. (Kyoto)*. **45**, 146–153 (2005).
48. Kawano, S., Nakao, T. & Hiraga, K. Induction of hepatic microsomal monooxygenases in female rats given various substituted phenols and hydroquinones. *Japan J. Pharmacol.* **31**, 459–462 (1981).

49. National Library of Medicine (US). 2,6-di-t-butyl-benzoquinone; Hazardous Substances Databank Number: 2775. (2002). Available at: <http://toxnet.nlm.nih.gov/cgi-bin/sis/search2/r?dbs+hsdb:@term+@DOCNO+2775>. (Accessed: 4th December 2018)
50. Taylor, J., Abadin, H., Hicks, H., Tarrago, O. & Cronin, D. Toxicological Profile for Ethylbenzene. *Agency Toxic Subst. Dis. Regist.* 341 (2010). doi:<http://dx.doi.org/10.1155/2013/286524>
51. Chan, P. C., Hasemani, J. K., Mahleri, J. & Aranyi, C. Tumor induction in F344/N rats and B6C3F1 mice following inhalation exposure to ethylbenzene. *Toxicol. Lett.* **99**, 23–32 (1998).
52. National Library of Medicine (US). Alpha-methyl styrene; Hazardous Substances Databank Number: 196. (2002). Available at: <http://toxnet.nlm.nih.gov/cgi-bin/sis/search2/r?dbs+hsdb:@term+@DOCNO+196>. (Accessed: 17th December 2018)
53. Fisher Scientific. 2-Phenyl-2-propanol; SDS [Online]. (2012). Available at: <https://www.fishersci.com/store/msds?partNumber=AC130830050&productDescription=2-PHENYL-2-PROPANOL+98%2B%25+5G&vendorId=VN00032119&countryCode=US&language=en>. (Accessed: 17th December 2018)
54. National Library of Medicine (US). 2-Phenylisopropanol; Hazardous Substances Databank Number: 5718. (2002). Available at: <http://toxnet.nlm.nih.gov/cgi-bin/sis/search2/r?dbs+hsdb:@term+@DOCNO+5718>. (Accessed: 4th December 2018)
55. Rosemond, Z. *et al.* Toxicological Profile for Styrene. *U.S Public Heal. Serv. Agency Toxic Subst. Dis. Regist.* 283 (2010). doi:<http://dx.doi.org/10.1155/2013/286524>
56. Leibman, K. C. Metabolism and toxicity of styrene. *Environ. Health Perspect.* **11**, 115–119 (1975).
57. Jegaden, D. *et al.* Environmental Health Study of the neurobehavioural toxicity of styrene at low levels of exposure. 527–531 (1993).
58. National Library of Medicine (US). Tetramethylsuccinonitrile; Hazardous Substances Databank Number: 7193. (2005). Available at: <http://toxnet.nlm.nih.gov/cgi-bin/sis/search2/r?dbs+hsdb:@term+@DOCNO+7193>. (Accessed: 4th December 2018)

59. Ensslin, A. S. & Koller, M. F. Convulsions and hypoglycemia due to tetramethyl succinonitrile intoxication in the polyvinyl chloride (PVC) industry: A 4-year follow-up. *Int. J. Occup. Med. Environ. Health* **27**, 188–195 (2014).
60. National Library of Medicine (US). 4-Vinyl-1-cyclohexene; Hazardous Substances Databank Number: 2872. (2005). Available at: <http://toxnet.nlm.nih.gov/cgi-bin/sis/search2/r?dbs+hsdb:@term+@DOCNO+2872>. (Accessed: 17th December 2018)
61. Hoyer, P. B., Devine, P. J., Hu, X., Thompson, K. E. & Sipes, I. G. *Ovarian Toxicity of 4-Vinylcyclohexene Diepoxide: A Mechanistic Model. TOXICOLOGIC PATHOLOGY* **29**, (2001).
62. Bevan, C. *et al.* Subchronic toxicity of 4-vinylcyclohexene in rats and mice by inhalation exposure. *Toxicol. Sci.* **32**, 1–10 (1996).
63. United States Environmental Protection Agency. Conducting a Human Health Risk Assessment. (2017). Available at: <https://www.epa.gov/risk/conducting-human-health-risk-assessment>. (Accessed: 12th March 2018)
64. United States Environmental Protection Agency. Risk Assessment Guidelines. (2018). Available at: <https://www.epa.gov/risk/risk-assessment-guidelines>. (Accessed: 12th March 2018)
65. World Health Organization Regional Office for Europe. *WHO Guidelines for Indoor Air Quality: Selected Pollutants*. (2010).
66. United States Department of Energy Chemical Safety. Table 2: Protective Action Criteria (PAC) Rev. 28 based on applicable 60-minute AEGLs, ERPGs, or TEELs. (2018). Available at: <https://www.cas.org/cas->. (Accessed: 12th April 2018)
67. US EPA Integrated Risk Information System. *Acetophenone (CASRN 98-86-2) | IRIS | US EPA*. (1988).
68. US EPA Integrated Risk Information System. *Benzaldehyde (CASRN 100-52-7) | IRIS | US EPA*. (1988).
69. US EPA Integrated Risk Information System. *Cumene (CASRN 98-82-8) | IRIS | US EPA*. (1988).
70. US EPA Integrated Risk Information System. *Ethylbenzene (CASRN 100-41-4) | IRIS | US EPA*. (1987).
71. US EPA Integrated Risk Information System. *Styrene (CASRN 100-42-5) | IRIS | US EPA*. (1987).
72. Rubey, W. A. & Grant, R. A. Design aspects of a modular instrumentation system for thermal diagnostic studies. *Rev. Sci. Instrum.* **59**, 265–269 (1988).

73. Aleph Objects, I. *LulzBot™ TAZ 5 User Manual*. (2015).
74. Afinia 3D. *H400 User Manual*. (2017).
75. Ultimaker. *Ultimaker 3 Installation and user manual*. (2016).
76. Prusa Research. *3D Printing Handbook*. (2015).
77. FlashForge Corporation. *FlashForge Finder 3D Printer User Guide*. (2017).
78. Overberger, C. G., O'Shaughnessy, M. T. & Shalit, H. The Preparation of Some Aliphatic Azo Nitriles and their Decomposition in Solution. *J. Am. Chem. Soc.* **71**, 2661–2666 (1949).
79. SI Group. Product Safety Summary for 2,4-di-tert-butylphenol (2,4-DTBP). Available at: <https://www.sigroup.com/EHSPdf/24-DTBPGPS.pdf>. (Accessed: 2nd November 2018)
80. Zhu, X. Y., Lee, S. M., Lee, Y. H. & Frauenheim, T. Adsorption and desorption of an O₂ molecule on carbon nanotubes. *Phys. Rev. Lett.* **85**, 2757–2760 (2000).
81. Sorescu, D. C., Jordan, K. D. & Avouris, P. Theoretical Study of Oxygen Adsorption on Graphite and the (8,0) Single-walled Carbon Nanotube. *J. Phys. Chem. B* **105**, 11227–11232 (2001).
82. Zhang, S., Shao, T., Kose, H. S. & Karanfil, T. Adsorption of Aromatic Compounds by Carbonaceous Adsorbents: A Comparative Study on Granular Activated Carbon, Activated Carbon Fiber, and Carbon Nanotubes. *Environ. Sci. Technol.* **44**, 6377–6383 (2010).
83. Galano, A. Carbon nanotubes: Promising agents against free radicals. *Nanoscale* (2010). doi:10.1039/b9nr00364a
84. Watts, P. C. P. *et al.* Carbon nanotubes as polymer antioxidants. *J. Mater. Chem.* (2003). doi:10.1039/b211328g
85. Fenoglio, I. *et al.* Reactivity of carbon nanotubes: Free radical generation or scavenging activity? *Free Radic. Biol. Med.* (2006). doi:10.1016/j.freeradbiomed.2005.11.010
86. Erickson, K. L. & Oelfke, J. Effect of Ambient Oxygen Concentration on Thermal Decomposition of Polyurethanes Based on MDI and PMDI. in *ACS Symposium Series* 387–407 (2009). doi:10.1021/bk-2009-1013.ch023

Vita

Dean James Lay was born in Chico, California. He attended the University of California, Davis, and received a bachelor's degree in Environmental Toxicology, while working as an organic chemistry tutor, a peer advisor, and a student lab assistant along the way. His first job out of college was working as an environmental consultant in and around Sacramento, California. In 2016, Dean moved to Baton Rouge, Louisiana, where he soon began working as a research associate in the Environmental Sciences Department. In the fall of 2017 he switched out of his full-time research position and joined the department as a master's student. Upon completion of his degree, he plans to re-enter the workforce in the environmental industry.